

1 Prepared for Plant Physiology: Research Article

2 Research Area: Signaling and Response

3

4 **Selinene volatiles are essential precursors for maize defense promoting**
5 **fungal pathogen resistance**

6 Yezhang Ding^a, Alisa Huffaker^a, Tobias G. Köllner^b, Philipp Weckwerth^a,
7 Christelle A. M. Robert^c, Joseph L. Spencer^d, Alexander E. Lipka^e, Eric A.
8 Schmelz^{a,*}

9 ^aSection of Cell and Developmental Biology, University of California at San
10 Diego, La Jolla, CA 92093-0380; ^bDepartment of Biochemistry, Max Planck
11 Institute for Chemical Ecology, Hans-Knöll-Straße 8, D-07745 Jena, ^cInstitute of
12 Plant Sciences, University of Bern, Bern, CH-3013 Switzerland, ^dIllinois Natural
13 History Survey, University of Illinois, Champaign, IL 61820; ^eDepartment of Crop
14 Sciences, University of Illinois, Urbana, IL 61801.

15

16 **Running title:** Selinene volatiles underlay antifungal defenses

17

18 **One Sentence Summary:** Maize terpene synthase 21 encodes a β -selinene
19 synthase enabling the production of antifungal defenses.

20 **List of Author contributions:**

21 E.A.S., A.H. and Y.D. conceived the original screening and research plans; Y.D.
22 performed most of the experiments; P.W. provided technical assistance to Y.D.;
23 Y.D., T.G.K., C.A.M.R., J.L.S., A.E.L. designed the experiments and analyzed
24 the data; E.A.S, Y.D. and A.H. conceived the project and wrote the article with
25 contributions of all the authors; T.G.K., C.A.M.R., A.E.L. supervised and
26 complemented the writing of specific sections.

27 ***Corresponding author:** Dr. Eric Schmelz; E-mail: eschmelz@ucsd.edu

28

29 **Funding sources:** E.A.S. and A.H. gratefully acknowledge support by startup
30 funds through the University of California San Diego, the DOE Joint Genome
31 Institute Community Science Program (grant #WIP 2568) and partial support for
32 this work through a NSF-IOS Competitive Award (#1139329).

33

34

35

36

37

38

39

40

41

42

43

44

45

46 **Abstract**

47 To ensure food security, maize (*Zea mays*) is a model crop for understanding
48 useful traits underlying stress resistance. In contrast to foliar biochemicals, root
49 defenses limiting the spread of disease remain poorly described. To better
50 understand below-ground defenses in the field, we performed root metabolomic
51 profiling and uncovered unexpectedly high levels of the sesquiterpene volatile β -
52 selinene and the corresponding non-volatile antibiotic derivative, β -costic acid.
53 The application of metabolite-based Quantitative Trait Loci (mQTL) mapping
54 using bi-parental populations, genome wide association studies, and near-
55 isogenic lines (NILs) enabled the identification of terpene synthase 21 (*ZmTps21*)
56 on chromosome 9 as a β -costic acid pathway candidate gene. Numerous closely
57 examined β -costic acid deficient inbred lines were found to harbor *Zmtps21*
58 pseudo genes lacking conserved motifs required for farnesyl diphosphate (FPP)
59 cyclase activity. For biochemical validation, a full length *ZmTps21* was cloned,
60 heterologously expressed in *E. coli* and demonstrated to cyclize FPP yielding β -
61 selinene as the dominant product. Consistent with microbial defense pathways,
62 *ZmTps21* transcripts strongly accumulate following fungal elicitation. Challenged
63 field roots containing functional *ZmTps21* alleles displayed β -costic acid levels
64 over $100 \mu\text{g g}^{-1}$ FW, greatly exceeding *in vitro* concentrations required to inhibit
65 the growth of five different fungal pathogens and rootworm larvae (*Diabrotica*
66 *balteata*). *In vivo* disease resistance assays, using *ZmTps21* and *Zmtps21* NILs,
67 further support the endogenous antifungal role of selinene-derived metabolites.
68 Involved in the biosynthesis of non-volatile antibiotics, *ZmTps21* exists as a
69 useful gene for germplasm improvement programs targeting optimized biotic
70 stress resistance.

71

72

73

74 **Introduction**

75 Plants are protected from a broad range of harmful biotic agents by initial
76 perception events, signal transduction cascades and the elicitation of defense
77 metabolism (Vanetten et al., 1994; Harborne, 1999; Dangl et al., 2013; Huffaker
78 et al., 2013). In maize (*Zea mays*), seedlings are largely protected from attack by
79 a complex suite of hydroxamic acid-based defenses, termed benzoxazinoids
80 (BX), responsible for resistance to diverse threats spanning fungal pathogens
81 and herbivores including Northern corn leaf blight (*Setosphaeria turtica*) and the
82 European corn borer (ECB; *Ostrinia nubilalis*) (Beck et al., 1957; Couture et al.,
83 1971; McMullen et al., 2009). Sixty years of research has resulted in a nearly
84 complete metabolic and genetic BX pathway in maize involving over a dozen
85 individual enzymes and metabolites (Frey et al., 2009; Meihls et al., 2013;
86 Handrick et al., 2016). Additionally, diverse terpenoids and underlying terpene
87 synthases (Tps) have also been demonstrated to play important protective roles
88 (Degenhardt, 2009; Schmelz et al., 2014). As indirect defenses, herbivore-
89 elicited terpene volatiles can function as diffusible signals to attract natural
90 enemies, such as parasitoids and entomopathogenic nematodes, to above- and
91 below-ground insect pests, respectively (Rasmann et al., 2005; Schnee et al.,
92 2006).

93 Of the many biosynthetic classes of natural products, terpenoids are the
94 most structurally diverse with well over 25,000 established compounds. In
95 addition to roles as phytohormone signals, specialized terpenoids mediate inter-
96 organism interactions and serve as chemical barriers (Gershenzon and
97 Dudareva, 2007). In maize, terpene olefins are nearly ubiquitous components of

98 induced above and below-ground volatile emissions acting as indirect plant
99 defenses following biotic stress (Turlings et al., 1990; Degenhardt, 2009;
100 Degenhardt et al., 2009; Kollner et al., 2013). Maize terpene olefins can also
101 serve as precursors for localized production of non-volatile antibiotic terpenoid
102 defenses (Schmelz et al., 2014). While often undetectable at the level of volatile
103 pathway intermediates, the inducible accumulation of non-volatile terpenoid end-
104 products can limit the damage caused by fungi, herbivores and oxidative
105 stresses (Harborne, 1999; Ahuja et al., 2012). Despite significant advances,
106 continuing discoveries in maize reveals that our collective knowledge of
107 biochemical defenses and pathway genes responsible for mitigating crop stress
108 remains incomplete.

109 Decades of intensive research in related Poaceous crops, such as rice
110 (*Oryza sativa*), has revealed multiple pathways of inducible labdane-related
111 diterpenoids including momilactones, oryzalexins, and phytocassanes that
112 underlay protective responses to biotic and abiotic stress (Schmelz et al., 2014).
113 More recently, complex arrays of acidic terpenoids have been detected in maize
114 and include sesquiterpenoids derived from β -macrocarpene and diterpenoids
115 derived from *ent*-kauranes, termed zealexins and kauralexins, respectively
116 (Huffaker et al., 2011; Schmelz et al., 2014). From a biosynthetic and pathway
117 perspective, maize genes underlying the production of antifungal agents remain
118 largely unknown. In the case of maize diterpenoid defenses, a specific *ent*-
119 copalyl diphosphate synthase (Anther ear 2; ZmAn2), is the only enzyme

120 demonstrated *in planta* essential for kauralexin biosynthesis (Vaughan et al.,
121 2015).

122 To uncover further defense pathways, we employed targeted metabolomic
123 profiling on field grown maize roots naturally exposed to combinations of
124 herbivores and pathogens (Baldwin, 2012). Curiously, high levels of rarely
125 encountered eudesmane sesquiterpenoids including β -selinene and β -costic acid
126 dominated the chemical profiles of many samples. While not previously
127 associated with maize, β -costic acid is known from the Asteraceae family,
128 including false yellowhead (*Dittrichia viscosa*) and costus (*Saussurea costus*),
129 and has been utilized in extracts for potent antibiotic activities against diverse
130 organisms (Rao and Alvarez, 1981; Wu et al., 2006; Katerinopoulos et al., 2011).
131 Despite the diverse phylogenetic occurrence in nature, a specific pathway
132 predominantly leading to β -costic acid has not been described in plants. To
133 explore the maize β -costic acid pathway, combined genetic mapping approaches
134 with the intermated B73 x Mo17 (IBM) population of recombinant inbred lines
135 (RILs) (Lee et al., 2002), the Goodman diversity panel (Flint-Garcia et al., 2005),
136 and IBM near-isogenic lines (NILs) (Eichten et al., 2011) were used for
137 metabolite-based Quantitative Trait Loci (mQTL) mapping. Biochemical
138 characterization of the mQTL-identified Tps candidate utilized heterologous
139 expression in *E. coli* to confirm identification of a comparatively product-specific
140 β -selinene synthase. Transcript expression and metabolite analyses following
141 elicitation with multiple pathogens and western corn rootworm (WCR, *Diabrotica*
142 *virgifera virgifera*) larvae (Gray et al., 2009; Meinke et al., 2009; Miller et al.,

143 2009; Spencer et al., 2009; Tinsley et al., 2013) were used to assess pathway
144 activation. Concentrations of β -costic acid below those detected in field tissues
145 were then used to examine *in vitro* antibiotic activity against 5 fungal species.
146 Similarly, NILs were used to investigate *in vivo* root resistance following
147 challenge with *Fusarium verticillioides* and *Fusarium graminearum*. Collectively
148 our results support the existence of a previously unrecognized β -costic acid
149 pathway in maize that contributes to fungal pathogen resistance.

150

151 **RESULTS**

152 **Identification of α and β -selinene derived products as inducible maize**
153 **sesquiterpenoids that can influence generalist root herbivores.** Our previous
154 investigation of maize responses following stem herbivory and fungal elicitation
155 enabled the discovery of two distinct biosynthetic classes of inducible acidic
156 terpenoids (Huffaker et al., 2011; Schmelz et al., 2011). Similarly, experiments
157 examining maize root defenses elicited by banded cucumber beetle (*Diabrotica*
158 *balteata*) larvae and *F. verticillioides* infection confirmed shared responses in
159 diverse tissue types (Vaughan et al., 2015). Given that predominant defenses
160 change over ontogeny and that controlled lab experiments do not capture the full
161 suite of biotic stresses in nature (Kollner et al., 2004; Baldwin, 2012), we sought
162 to expand our targeted metabolomic analyses to roots in the context of natural
163 biotic challenge (Schmelz et al., 2004). As expected, mature visibly-necrotic roots
164 of field-challenged maize lines including hybrid sweet corn (var. Golden Queen)
165 and the inbred Mo17 contained zealexins (Fig. 1A); however, chemically

166 extracted samples unexpectedly also contained α -selinene, β -selinene, β -costol,
167 α -costic acid and β -costic acid (Fig. 1; Supplemental Fig. S1). In volatile
168 collections of live Mo17 root emissions, α -selinene, β -selinene (Fig. 2) and the
169 aldehyde β -costal (Supplemental Fig. S1) were likewise detectable. As the major
170 analyte, live field-collected Mo17 roots displaying visible necrosis emit
171 predominantly β -selinene (Fig. 2). In contrast, β -selinene emission is absent in
172 B73 roots; however, production reappears in select B73 x Mo17 RILs, for
173 example IBM0287 (Fig. 2). Similar volatile emission results are observed in live
174 Mo17 stems following inoculation with the necrotrophic fungal pathogen
175 (*Cochliobolus heterostrophus*), commonly known as southern leaf blight (SLB)
176 (Fig. 2). Consistent with root metabolite patterns, the reference genome inbred
177 B73 (Schnable, 2009) remains void of α and β -selinene stem volatiles under
178 identical conditions (Fig. 2). Qualitative metabolite differences between B73,
179 Mo17 and select RILs provides empirical evidence for genetic variation in
180 selinene biosynthesis and encourages the use of genetic mapping resources
181 (Lee et al., 2002).

182 Our quantification of unexpectedly high levels of β -selinene and β -costic
183 acid in field collected maize roots was paired with casual field observations of
184 adult *D. balteata* beetles on leaves. Given the broad host range of *D. balteata*
185 larvae (Saba, 1970) and pest pressures exerted by western corn rootworm
186 (WCR: *Diabrotica virgifera virgifera*) larvae including the promotion of secondary
187 disease (Flint-Garcia et al., 2009; Gray et al., 2009), we conducted controlled
188 *Diabrotica-maize* interaction experiments. In growth chamber assays, tissue

189 extracts of roots revealed both β -selinene and β -costic acid following damage by
190 WCR larvae (Fig. 2). Given the high levels of selinene-derived metabolites
191 observed in field-collected roots, additional assessments of WCR and *D. balteata*
192 preference and performance were conducted on larvae. For both *Diabrotica*
193 species, we observed no influence of exogenously applied β -costic acid on root
194 preference but found a significant inhibitory role of β -costic acid on *D. balteata*
195 performance (Fig. 2).

196

197 **Combined linkage and association mapping identifies maize terpene**
198 **synthase *ZmTps21* as a candidate biosynthetic gene.** β -selinene has been
199 previously detected in the volatile profiles of pathogen-challenged maize tissue;
200 however, the biosynthetic source and physiological function(s) have not been
201 elucidated (Becker et al., 2014). Given our observation that selinene-derived
202 pathway products can predominate in maize under specific conditions, we sought
203 to identify the gene(s) responsible. We first employed the IBM-RILs for mQTL
204 mapping. As a predictable non-volatile pathway end product, β -costic acid levels
205 were analyzed in naturally challenged roots of 216 IBM RILs (Supplemental
206 Table S1). Composite Interval Mapping (CIM) placed the locus in Bin 9.05 (Fig.
207 3) (Gardiner et al., 1993). For comparative purposes, the IBM-RIL data was also
208 explored using 173,984 SNPs and association mapping via a General Linear
209 Model (GLM) (Bradbury et al., 2007) and Unified Mixed Linear Model (MLM) (Yu
210 et al., 2006). All approaches supported a single statistically significant locus on
211 chromosome 9 (Fig. 3, Supplemental Fig. S2). Additionally we performed an

212 elicited metabolite-based Genome-Wide Association Study (mGWAS) using β -
213 costic acid levels in greenhouse grown inbreds from the Goodman diversity panel
214 (Flint-Garcia et al., 2005). Similarly, we detected a single statistically significant
215 locus on chromosome 9 (Fig. 3). An independent mGWAS replication conducted
216 with field grown plants yielded an identical result (Supplemental Fig. S2).
217 Correspondence of physical QTL coordinates identified with IBM RILs and the
218 replicated GWAS results (Fig. 3, Supplemental Fig. S2) robustly supported a
219 single narrow locus controlling maize β -costic acid levels.

220 For additional confirmation, select B73 \times Mo17 near isogenic lines (NILs)
221 were analyzed following stem elicitation (Eichten et al., 2011). B73 chromosomal
222 segments introgressed into Mo17 dominating lines (specifically m012, m048,
223 m050 and m062) were each deficient in the production of β -costic acid (Fig. 3). In
224 contrast, β -costic acid production in NILs with introgressions of the Mo17 allele
225 into the B73 genetic background (lines b047, b055, b069, and b157) were similar
226 to Mo17 (Fig. 3, Supplemental Fig. S3), confirming existence of the β -costic acid
227 associated locus in Bin 9.05. Further analyses of additional NIL lines (b022,
228 b033, m002, m065, and m092) narrowed the locus to 13 predicted genes
229 isolated on bacterial artificial chromosome (BAC) clones, AC213878 and
230 AC204415 (Fig. 3). Of the remaining candidates, only a single uncharacterized
231 gene (GRMZM2G011151) displayed significant sequence homology with known
232 terpene synthases. Supportively, detailed examination of 3 independent
233 association mapping results likewise demonstrated the presence of highly
234 significant SNPs associated with the Tps candidate (GRMZM2G011151), termed

235 *ZmTps21* (Supplemental Fig. S2). Genomic structure analysis of B73 *Zmtps21*
236 revealed three predicted exons encoding a 297 amino acid protein lacking the
237 conserved Tps catalytic domains, namely the DDXXD and RXR motifs (Fig. 3),
238 which are essential for function (Chen et al., 2011). Collectively, these findings
239 made B73 *Zmtps21* a parsimonious inactive β -selinene synthase pseudogene
240 candidate meriting further examination.

241 In an attempt to isolate the Mo17 *ZmTps21* cDNA sequence, early RT-
242 PCR trials with primers based upon B73 *Zmtps21* cDNA failed due to nucleotide
243 polymorphisms. Eventually a segment near the Mo17 *ZmTps21* 5'-end of
244 genomic DNA of was obtained by a PCR and sequenced. Alignments revealed
245 that the segment near the Mo17 *ZmTps21* 5'-end DNA fragment shared high
246 sequence similarity to that of B73 *Zmtps21*. Therefore, the 5'-end cDNA
247 sequence of Mo17 *ZmTps21* was obtained by RT-PCR and extended by PCR
248 with rapid amplification of cDNA ends (rPCR) using a cDNA library to obtain the
249 full-length Mo17 *ZmTps21* cDNA (Fig. 3; Supplemental Fig. S4). The deduced
250 amino acid sequence of the open reading frame contained the conserved
251 terpene synthase domains including the DDXXD (residues 325 to 329) and RXR
252 (residues 288 to 290) motifs (Supplemental Fig. S4). The amino acid sequence
253 of *ZmTps21* resembles (<60% identity) those of other plant sesquiterpene
254 synthases and shares less than 40% sequence identity with previously
255 characterized maize sesquiterpene synthases, such as *ZmTps6*, *ZmTps10*,
256 *ZmTps11*, and *ZmTps23* (Supplemental Fig. S4). With only 30% identity at the
257 amino acid level, Mo17 *ZmTps21* is even more distantly related to the *Ocimum*

258 *basilicum* sesquiterpene synthase (SES) which produces detectable levels of β -
259 selinene as part of a complex blend (Supplemental Fig. S4) (Iijima et al., 2004).

260 To understand the extent of genetic variation in *ZmTps21* alleles, we
261 examined 15 commonly investigated inbreds. *ZmTps21* genomic sequences
262 were isolated by PCR using primers based on the B73-*Zmtps21* and Mo17-
263 *ZmTps21* genome sequences, respectively (Supplemental Table S1). Sequence
264 analyses demonstrated that the *Zmtps21* alleles from B73-like lines (Ki3, M37W,
265 MS71, M162W, CML247, Ki11, Mo18W) share >98% DNA sequence identity and
266 basic genome structure, whereas Mo17-like *ZmTps21* alleles (Hp301, TX303,
267 Oh43, Oh7B, Ky21 and W22) contain six exons and share higher than 98%
268 sequence identity at the amino acid level (Supplemental Fig. S5 and S6). These
269 results support the hypothesis that B73-like inbred lines share a common
270 mutation ancestry.

271

272 ***In vitro* assays demonstrate that ZmTps21 is a largely product-specific β -**
273 **selinene synthase.** *ZmTps21* lacks a predicted N-terminal transit peptide
274 suggesting that the enzyme is not targeted to plastids as is typical of
275 monoterpene and diterpene synthases, but instead remains cytosolic consistent
276 with predictions for a sesquiterpene synthase (Gershenzon, 1999). To obtain
277 additional support for the hypothesis that Mo17 *ZmTps21* is a β -selinene
278 synthase, heterologous expression was performed in *E. coli* and the resulting
279 protein extract was incubated with the precursor substrate (*E,E*)-farnesyl
280 diphosphate (FPP). β -selinene is the dominant product observed by GC-MS

281 along with several other minor sesquiterpene olefins, including α -selinene and β -
282 elemene (Fig. 4). Thus *ZmTps21* encodes a selinene synthase with predominant
283 β -selinene product specificity that includes α -selinene as a minor product
284 consistent with the olefin and oxygenated metabolite ratios observed *in planta*
285 (Fig. 1, Supplemental Fig. S1). Injection of the *ZmTps21* reaction products on a
286 GC column at different temperatures revealed that the β -elemene present is due
287 to a Cope rearrangement of germacrene A (Supplemental Fig. S7 and S8) (de
288 Kraker et al., 2001). Germacrene A also is a neutral reaction intermediate of the
289 tobacco (*Nicotiana tabacum*) enzyme 5-*epi*-aristolochene synthase (TEAS)
290 responsible for the pathogen-elicited biosynthesis of capsidiol (Cane, 1990;
291 Starks et al., 1997). The enzymatic protonation of germacrene A leads to the
292 eudesmane carbocation further converted to 5-*epi*-aristolochene. Given that β -
293 selinene is simply formed by a deprotonation of a eudesmane carbocation, it
294 likely that the reaction catalyzed by *ZmTps21* also includes the formation and
295 protonation of germacrene A. A sequence comparison of *ZmTps21* with TEAS
296 and other Tps able to protonate neutral reaction intermediates demonstrate that
297 the amino acids of the catalytic triad involved in the protonation reaction are
298 conserved (Starks et al., 1997) (Supplemental Fig. S4). Curiously, two *ZmTps21*
299 mutants with altered C-termini obtained as cloning artifacts produced only
300 germacrene A (Supplemental Fig. S7 and S8), suggesting additional influence of
301 the C-terminus on the protonation reaction and specificity of the final product.
302

303 ***ZmTps21* transcripts are pathogen inducible and correspond with β -costic**
304 **acid accumulation.** To examine endogenous patterns, we compared Mo17
305 *ZmTps21* expression with established *ZmTps6/11* expression associated with
306 zealexin biosynthesis (Kollner et al., 2008; Huffaker et al., 2011). Similar to
307 *ZmTps6/11*-zealexin relationships, *ZmTps21* transcripts and β -costic acid are
308 barely detectable in control tissues and not significantly elicited by mechanical
309 damage alone (Fig. 5). After elicitation with heat-killed *Fusarium* hyphae,
310 *ZmTps6/11* transcripts reached maximal levels at day 1 while *ZmTps21*
311 transcripts levels continued to accumulate for an additional day (Fig. 5). Zealexin
312 A1 was readily detectable at day 1 and continued to increase over the 4 days
313 while β -costic acid accumulation was first detected at day 2 reaching similar
314 levels at day 4 (Fig. 5). Thus, *ZmTps21* transcripts and product accumulation
315 display longer-term and temporally layered elicitation kinetics alongside the
316 zealexin biosynthetic pathway.

317 To examine whether *ZmTps21* transcripts and β -costic acid levels change
318 specifically in response to aggressive pathogens such as *C. heterostrophus* and
319 *F. verticillioides* or whether the response also follows opportunistic fungi such as
320 *Rhizopus microsporus* and *Aspergillus parasiticus*, both parameters were
321 analyzed in inoculated stems. Exposure to *C. heterostrophus*, *F. verticillioides*, *R.*
322 *microsporus*, and *A. parasiticus* all resulted in significant induction of both
323 *ZmTps6/11* transcript levels and zealexin A1, which vary in response to different
324 fungi (Fig. 5) (Huffaker et al., 2011). In the same context the 4 fungal species
325 also led to significant accumulation of *ZmTps21* transcripts and β -costic acid

326 (Fig. 5). Infection with *C. heterostrophus* led to the highest induction of both
327 *ZmTps21* transcripts and β -costic acid in stems, similar to *ZmTps6/11* transcripts
328 and zealexin levels, respectively (Fig. 5). To further consider the natural
329 occurrence of β -selinene derived metabolites in diverse inbreds (McMullen et al.,
330 2009) we analyzed the scutella tissues of 10-d old seedling plants. β -costic acid
331 was detected in all lines harboring Mo17-like *ZmTps21* alleles (Hp301, TX303,
332 Oh43, Oh7B, Ky21, and W22) and was comparatively absent from all inbreds
333 harboring B73-like *Zmtps21* (Ki3, M37W, MS71, M162W, CML247, Ki11,
334 Mo18W) pseudogenes (Fig. 5; Supplemental Fig. S5 and S6). Collectively,
335 these results support the existence of a single β -selinene synthase in maize
336 responsible for the production of β -costic acid.

337

338 ***In vitro* and *in vivo* assays support a defensive role for β -costic acid in**

339 **fungal disease resistance.** In effort to assess physiological roles, we quantified
340 β -costic acid present in replications of field-collected roots of B73, Sweet corn
341 (var. Golden Queen), Mo17 and the *ZmTps21* IBM-RIL 0287. On average,
342 sectors of roots containing visible necrosis from each responsive line contained
343 well over 100 $\mu\text{g g}^{-1}$ FW of β -costic acid (Fig. 5). Using this conservative
344 baseline, we then examined the antimicrobial activity of β -costic acid against *F.*
345 *verticillioides*, *F. graminearum*, *R. microsporus*, *A. parasiticus*, and *C.*
346 *heterostrophus* in liquid culture assays. At 100 $\mu\text{g ml}^{-1}$, β -costic acid completely
347 inhibited the growth of *R. microsporus* and significantly suppressed the growth of
348 all other fungi (Fig. 6; Supplemental Fig. S9). Importantly, β -costic acid

349 concentrations as low as 25 $\mu\text{g ml}^{-1}$ retained significant inhibitory activity in each
350 case demonstrating that β -costic acid has the potential to function as wide-
351 spectrum antifungal defense at low doses. To estimate *in vivo* roles, mature roots
352 of greenhouse grown B73, Mo17 and 2 predominantly Mo17 IBM-NILs
353 (Supplemental Fig. S9) were damaged and treated with either H₂O or H₂O
354 containing spores of *F. verticillioides* and *F. graminearum* separately. Seven
355 days later, the B73 inbred and the IBM-NIL (m050) harboring a *Zmtps21*
356 pseudogene displayed significantly greater levels of disease as estimated by
357 *Fusarium* DNA levels compared to Mo17 and the functional *ZmTps21* IBM-NIL
358 (m065) (Fig. 6). Collectively, our results are consistent with ZmTps21 pathway
359 products as mediators of antifungal defenses.

360

361 **Discussion**

362 Maize biochemicals either demonstrated or predicted to mediate insect
363 and pathogen defense include diverse volatiles (Degenhardt, 2009; Degenhardt
364 et al., 2009), benzoxazinoids (Frey et al., 2009; Ahmad et al., 2011; Meihls et al.,
365 2013; Handrick et al., 2016), flavonoids and C-linked flavonoid glycosides (Meyer
366 et al., 2007; Balmer et al., 2013; Casas et al., 2016), non-protein amino acids
367 (Yan et al., 2015), oxylipins (Christensen et al., 2015; Borrego and Kolomiets,
368 2016), and non-volatile terpenoids (Schmelz et al., 2014). Among all biosynthetic
369 classes, terpenoids are the most diverse structurally and in demonstrated
370 breadth of ecological interactions mediated (Gershenzon and Dudareva, 2007).
371 At the genome level, plants commonly possess mid-sized terpene synthase gene

372 families ranging from 14 to 70 members (Chen et al., 2011). More specifically, in
373 maize use of “terpene” as a keyword search in Phytozome
374 (<https://phytozome.jgi.doe.gov>) currently reveals more than 30 *Tps* gene models.
375 Collective efforts have resulted in the genetic, biochemical and ecological
376 characterization of approximately half of the maize enzymes encoded by *Tps*
377 with product specificity in the production of mono-, sesqui- and diterpenes
378 (Schnee et al., 2002; Kollner et al., 2004; Schnee et al., 2006; Kollner et al.,
379 2008; Degenhardt et al., 2009; Fu et al., 2016; Richter et al., 2016). Maize
380 terpene volatiles are often highly inducible following insect attack and aid in the
381 attraction of diverse natural enemies both above and below ground (Turlings et
382 al., 1990; Rasmann et al., 2005; Degenhardt et al., 2009). Oxygenated non-
383 volatile terpenoids can also accumulate and act as antifungal agents and insect
384 antifeedants (Schmelz et al., 2011). As part of this biochemical complexity, we
385 demonstrate that maize tissues are capable of accumulating both high levels of
386 the sesquiterpene olefin β -selinene and the corresponding non-volatile
387 oxygenated derivative termed β -costic acid. Intriguingly, β -costic acid is produced
388 in diverse aromatic and medicinal plants widely investigated for bioactive agents
389 driving antibiotic and anti-arthropod activities (Rao and Alvarez, 1981; Wu et al.,
390 2006; Katerinopoulos et al., 2011). Despite the widespread occurrence in nature,
391 *Tps* essential for the specific *in vivo* production of β -costic acid have not been
392 previously demonstrated *in planta*. We currently describe a maize β -selinene
393 synthase, termed ZmTps21, which is required for the inducible accumulation of
394 β -costic acid.

395 High tissue concentrations of β -costic acid were first detected in mature
396 field-collected roots of both sweet corn and Mo17 but appeared absent the B73
397 inbred. Use of complimentary mapping resources and the induced production of
398 β -costic acid as a qualitative trait demonstrated single a narrow QTL containing a
399 *Tps* gene candidate.

400 To examine the full-length Mo17 *ZmTps21* allele identified, heterologous
401 expression experiments were conducted in *E. coli* and protein extracts incubated
402 with FPP yielded β -selinene as the dominant volatile product. Based on
403 numerous inbred lines and predicted proteins from genome sequences
404 (Supplemental Fig. S5 and S6), the *in vitro* products of functional *ZmTps21* are
405 consistent with the endogenous presence of β -costic acid in all Mo17-like
406 *ZmTps21* lines and likewise an absence in all B73-like *Zmtps21* lines (Fig. 5).

407 Precursors of dominant biochemical defense pathways are commonly the
408 products of fully functional duplicate genes (Kollner et al., 2008; McMullen et al.,
409 2009); however, mGWAS mapping results (Fig. 2) and the exclusive presence of
410 β -costic acid (Fig. 5) in lines with full-length *ZmTps21* alleles collectively support
411 the existence of a single maize β -selinene synthase. At the enzymatic level, the
412 existence of a product specific β -selinene synthase was first reported in 1992
413 through the examination of *Citronella mitis* fruits; however, the specific *Tps* gene
414 responsible remains unknown (Belingheri et al., 1992). Acid-induced cyclization
415 of germacrenes can also yield selinenes making it highly probable that a
416 germacrene A synthase is responsible for the costol, costal, and costic acid
417 eudesmanes in costus root oil; however, it remains unknown if costus contains a

418 specific β -selinene synthase (de Kraker et al., 2001). Further elucidation of the β -
419 costic acid pathway will require the discovery of a yet unresolved cytochrome
420 P450 monooxygenase(s) performing sequential oxidations leading to the
421 carboxylic acid. Characterized germacrene A oxidases from the Asteraceae drive
422 the biosynthesis of germacrene A acid which following acid-induced
423 rearrangement can yield blends that include β -costic acid (Nguyen et al., 2010).
424 A related P450 that directly oxidizes β -selinene to yield β -costic acid is predicted
425 to occur in maize yet remains unknown.

426 While numerous plants in nature constitutively make β -selinene in specific
427 tissues and life stages, β -selinene is rarely detected in maize and has occurred
428 only in the context of pathogen attack (Becker et al., 2014; Sowbhagya, 2014).
429 Consistent with this observation we find *ZmTps21* transcripts largely
430 undetectable in healthy control tissues or those experiencing simple mechanical
431 damage (Fig. 5). In contrast, heat-killed *Fusarium* hyphae and a wide range of
432 live fungal species elicit *ZmTps21* transcript accumulation and β -costic acid
433 production. With conceptual similarities to the zealexin pathway, the elicitation
434 kinetics of both *ZmTps21* transcripts and β -costic acid differ and are temporally
435 behind those of *ZmTps6/11* and zealexins. Given the broader range of fungi
436 species displaying β -costic acid mediated growth suppression at $25 \mu\text{g ml}^{-1}$
437 compared to similar assays using zealexins (Huffaker et al., 2011), it is possible
438 that the *ZmTps21* pathway exists as an additional potent line of defense
439 activated sequentially as maize plants experience sustained attack. If this
440 hypothesis is true, related studies on maize disease resistance should note

441 biological roles for QTLs that include *ZmTps21*. Supportively, independent
442 disease-related QTLs have been detected in broad regions spanning Bin 9.05
443 (Baumgarten et al., 2007; Berger et al., 2014). More specifically *ZmTps21*
444 (GRMZM2G011151) has been identified as uniquely present in transcriptome
445 analyses of resistant inbred lines associated with enhanced antifungal defenses
446 (Lanubile et al., 2014). In an empirical assessment of the *in vivo* role of
447 *ZmTps21* derived defenses, root experiments using B73, Mo17 and 2 Mo17 NILs
448 support the suppression of both *F. graminearum* and *F. verticillioides* growth in
449 lines carrying functional Mo17 *ZmTps21* alleles (Fig. 6). Most maize biochemical
450 defenses likely function in the context of complex arrays of bioactive metabolites
451 from numerous pathways. In this context, isogenic mutants in numerous inbred
452 backgrounds would be an ideal and improved platform for the critical examination
453 of *ZmTps21* mediated biological functions. While the present study does not
454 accomplish this long-term goal, we provide a foundation and mechanistic
455 justification for related research directions.

456 Curiously, of lines closely examined at the gene level, β -costic acid
457 biosynthesis mediated by *ZmTps21* is associated with inbreds originating from
458 U.S. breeding programs. In contrast, β -costic acid biosynthetic capacity is largely
459 absent from more geographically diverse accessions. It is tempting to speculate
460 that while the β -costic acid pathway is commonly absent due to a partial gene
461 deletion, *ZmTps21* may have been maintained by positive selection during the
462 breeding of U.S. maize lines. Western corn rootworm (WCR: *Diabrotica virgifera*
463 *virgifera*) larvae exist as a candidate pest pressure known to devastate the roots

464 of temperate maize through below-ground herbivory and the promotion of
465 secondary disease (Flint-Garcia et al., 2009; Gray et al., 2009). In growth
466 chamber experiments, maize plants containing a functional *ZmTps21* allele
467 produced both β -selinene and β -costic acid following damage by WCR larvae
468 (Fig. 2). Consistent with a long-term association, unlike the generalist *D. balteata*,
469 WCR larvae were not significantly affected in preference or performance by β -
470 costic acid as a direct defense (Fig. 2). In this context, β -costic acid is likely to be
471 more important in limiting the secondary spread of fungal pathogens promoted by
472 root herbivory. However, while not specifically examined here, we speculate that
473 root pools of β -selinene may serve as a volatile attractant to natural enemies of
474 *Diabrotica* larvae such as entomopathogenic nematodes (Rasmann et al., 2005;
475 Degenhardt et al., 2009). This phenomena has been demonstrated in context of
476 trace amounts of maize root caryophyllene elicited following WCR larval
477 herbivory. More broadly, numerous root terpene volatiles can attract both
478 entomopathogenic and phytopathogenic nematodes, a result that highlights
479 complex tradeoffs in the deployment of rhizosphere signals (Ali et al., 2011).

480 In conclusion, our current study identifies the presence of numerous α/β -
481 selinene derived metabolites in maize tissues following biotic stress. In numerous
482 trials using select maize lines, β -selinene and β -costic acid exist as predominant
483 *ZmTps21*-derived terpenoids produced following fungal elicitation, long-term root
484 herbivory and combined field pressures. Antifungal assays using both *in vitro* and
485 *in vivo* approaches support an antifungal defense role for *ZmTps21* pathway
486 products. Root herbivores are likely to be additionally impacted given that β -

487 costic acid can reduce the performance of generalists such as *D. balteata* in
488 controlled bioassays. The discovery of further immune-related biochemical traits
489 is certain to continue given the extreme genetic diversity in maize highlighted by
490 over 8000 representative transcript assemblies detectable in diverse germplasm
491 that are absent from B73 (Hirsch et al., 2014). To fill existing voids highlighted by
492 comparative genomics, the combined application of metabolomics, mapping, and
493 *in vitro* biochemistry provides a useful approach to rapidly connect phenotypes
494 with genotypes (Meihls et al., 2013; Handrick et al., 2016; Richter et al., 2016).
495 Our current identification of ZmTps21 as a β -selinene synthase required for β -
496 costic acid production adds to the foundational knowledge of useful maize
497 biochemical pathways that can be intentionally combined for combating complex
498 biotic pressures.

499

500 **MATERIALS AND METHODS**

501 **Plant and Fungal Materials**

502 Seeds of the Intermated B73×Mo17 (IBM) population of recombinant inbred lines
503 (RILs) and the Goodman diversity panel (Flint-Garcia et al., 2005) were kindly
504 provided by Dr. Peter Balint-Kurti (USDA-ARS, Raleigh, NC, USA) and Dr. Georg
505 Jander (Boyce Thompson Institute, Ithaca, NY, USA) (Supplemental Table S2).
506 The IBM-RILs and Goodman diversity panel (replicate 2) were planted at the
507 Biology Field Station located on the University of California San Diego (UCSD)
508 campus in La Jolla, CA, USA, during the summers of 2015 and 2016,
509 respectively. Field challenged roots from B73, Mo17, hybrid sweet corn (*Zea*

510 *mays* var. Golden Queen; Southern States Cooperative, Inc. Richmond, VA,
511 USA) and IBM RILs were recovered 70 days after planting, washed, frozen in
512 liquid N₂, ground to a fine powder and ultimately used for genetic mapping.
513 Seeds of indicated B73×Mo17 near-isogenic lines (provided by the Maize
514 Genetic COOP Stock Center, Urbana, IL, USA), landrace inbreds (B73, Ki3,
515 M37W, Ms71, M162W, CML247, Ki11, Mo18W, Hp301, TX303, Oh43, Oh7B,
516 Ky21, Mo17, and W22; National Genetic Resources Program, Germplasm
517 Resources Information Network, Ames, IA) were germinated in MetroMix 200
518 (Sun Gro Horticulture Distribution, Inc.) supplemented with 14-14-14 Osmocote
519 (Scotts Miracle-Gro) and grown in a greenhouse as previously described
520 (Schmelz et al., 2009) (Supplemental Table S2). Fungal stock cultures of
521 *Rhizopus microsporus* (Northern Regional Research Laboratory stock no.
522 54029), *Fusarium verticillioides* (Northern Regional Research Laboratory; NRRL
523 stock no. 7415), *Fusarium graminearum* (NRRL stock no. 31084) *Aspergillus*
524 *parasiticus* (nor-1), and *Cochliobolus heterostrophus* were grown on V8 agar for
525 12 days before the quantification and use of spores (Huffaker et al., 2011;
526 Huffaker et al., 2013). Heat-killed *Fusarium venenatum* (strain PTA-2684)
527 hyphae was commercially obtained (Monde Nissin Corporation Co.) and used
528 safely for large-scale field mGWAS trials as a non-infectious elicitor lacking
529 known *Fusarium* mycotoxins.

530

531

532 **Genetic Mapping of *ZmTps21***

533 Using the presence of β -costic acid in necrotic tissues as a trait, the B73
534 *Zmtps21* locus was mapped using 216 IBM RIL lines (Lee et al., 2002) and
535 further supported using select B73xMo17 NILs (Eichten et al., 2011). Marker
536 data for the IBM RIL population were provided by Dr. Peter Balint-Kurti (USDA-
537 ARS, Raleigh, NC). Windows QTL Cartographer (Version 2.5;
538 <http://statgen.ncsu.edu/~shchwang/WQTLCart.htm>) was employed for metabolite
539 Quantitative Trait Locus (mQTL) analysis with composite interval mapping (CIM).
540 The WinQTLCart program was set as following: CIM program module=Model 6:
541 Standard Model, walking speed=1 cM, control marker numbers=5, window
542 size=10 cM, regression method=backward regression. Permutations (500) were
543 run to determine the $P < 0.05$ logarithm (base 10) of odds (LOD) significance
544 threshold (Churchill and Doerge, 1994). A list of RILs and NILs used for mapping
545 in this study are given in (Supplemental Table S2). In effort to confirm and
546 potentially refine the position of the mQTL identified using CIM, association
547 analyses were also conducted on the IBM RILs using the General Linear Model
548 (GLM) in TASSEL 5.0 (Bradbury et al., 2007) and the Unified Mixed Linear Model
549 (MLM) to effectively control for false positives arising from the differential
550 population structure and familial relatedness present in diversity panels (Yu et al.,
551 2006). Unlike diversity panels, differential population structure and familial
552 relatedness are not typically significant features in biparental RIL panels and thus
553 the GLM and MLM models were predicted to generate similar results in the IBM
554 RIL association analyses. Geneotypic data from imputed IBM RIL SNP markers
555 (July 2012 All Zea GBS final build; www.panzea.org) were used for association

556 analyses of root β -costic acid levels in the intermated B73 \times Mo17 (IBM)
557 population. 173,984 SNP markers with < 20% missing genotypes and minor
558 allele frequency (MAF) > 15% were used.

559 A metabolite based genome-wide association study (mGWAS) was
560 conducted for elicited levels β -costic acid as a trait in the Goodman diversity
561 panel (Flint-Garcia et al., 2005) using the Unified MLM in TASSEL 5.0 (Yu et al.,
562 2006; Bradbury et al., 2007). Final analyses were conducted with the R package
563 GAPIT (Zhang et al., 2010; Lipka et al., 2012), which involves EMMA (executed
564 by R package) and Compressed MLM (CMLM) population parameters previously
565 determined (P3D) to identify genomic regions putatively associated with the trait.
566 GWAS analyses utilized a B73 Version 2 referenced HapMap consisting of
567 246,477 SNPs previously derived from an Illumina 50K array (Cook et al., 2012)
568 and a genotyping by sequencing (GBS) strategy (Elshire et al., 2011) filtering
569 less than 20% missing genotype data with minor allele frequencies (MAF) > 5%
570 (Samayoa et al., 2015; Olukolu et al., 2016). The kinship matrix (K), estimated
571 from 246,477 SNPs was used jointly with population structure (Q) to improve
572 association analysis (VanRaden, 2008). All metabolite data were \log_2
573 transformed prior to statistical analysis to improve normality. The Quantile-
574 Quantile plots and Manhattan plots were constructed in the R package qqman
575 (<http://cran.r-project.org/web/packages/qqman>) (Turner, 2014).

576

577 **Identification and Quantification of Metabolites**

578 Unless otherwise stated, all maize tissue samples were rinsed with water, frozen
579 in liquid N₂, ground to a fine powder in a mortar and stored at -80 C for further
580 analyses. For Vapor Phase Extraction (VPE) based sample preparation, 50 mg
581 aliquots were first weighed, solvent extracted in bead homogenizer, and
582 derivatized using trimethylsilyldiazomethane as previously described (Schmelz et
583 al., 2004; Schmelz et al., 2011). GC-MS analysis was conducted using an Agilent
584 6890 Series gas chromatograph coupled to an Agilent 5973 mass selective
585 detector (interface temp, 250°C; mass temp, 150°C; source temp, 230°C;
586 electron energy, 70 eV). The GC was operated with a DB-35MS column (Agilent,
587 Santa Clara, USA, 30 m x 0.25 mm x 0.25 µm). The sample was introduced as a
588 splitless injection with an initial oven temperature of 45°C. The temperature was
589 held for 2.25 min, then increased to 300°C with a gradient of 20°C min⁻¹, and
590 held at 300°C for 5 min. GC/EI-MS based quantification of β-costic acid was
591 based upon the slope of an external standard curve constructed from β-costic
592 acid (Ark Pharm, #AK168379) spiked into 50 mg aliquots of frozen powdered
593 untreated maize stem tissues which were then processed using VPE (Schmelz et
594 al., 2004). In representative samples analyzed by GC/EI-MS, β-costol was
595 identified based 99% EI match within the Robert P. Adams essential oil MS
596 library (Allured Books). While not previously detected in maize, β-costol is an
597 anticipated intermediate in samples rich in both β-selinene and β-costic acid.

598 For headspace recovery of ZmTps21 enzyme products by solid phase
599 micro-extraction (SPME), fibers containing 100 µm polydimethylsiloxane
600 (SUPELCO, Belafonte, PA, USA) were placed into reaction vials for 60 min

601 incubations at 30°C and then introduced into the GC injector for the analyses of
602 the adsorbed reaction products. GC-MS analyses conducted on SPME samples
603 utilized a splitless injection, a DB-5MS column (Agilent, Santa Clara, USA, 30 m
604 x 0.25 mm x 0.25 µm) and an initial oven temperature of 80°C. The temperature
605 was held for 2 min, then increased to 240°C with a gradient of 7°C min⁻¹, and
606 further increased to 300°C with a gradient of 60°C min⁻¹ and a hold of 2 min.
607 Precise instrument settings of the Agilent 5973 mass selective detector were
608 identical to those stated above used for plant samples. For GC-MS analysis with
609 a cooler injector, the injector temperature was reduced from 240°C to 150°C.

610 Volatiles emitted from elicited stems and naturally challenged roots of field
611 grown plants were collected by passing purified air over the tissue samples at
612 600 ml min⁻¹ and trapped on inert filters containing 50 mg HayeSep® Q (80-100
613 µm mesh) polymer adsorbent (Sigma-Aldrich, St. Louis, MO, USA). Individual
614 samples were then eluted with 150 µl methylene chloride, and analyzed by GC
615 coupled with flame ionization detector (FID) as previously described (Schmelz et
616 al., 2001). β-selinene and related volatiles were quantified by GC-FID using the
617 slope of an external standard curve of (*E*)-β-farnesene. Select samples were
618 analyzed by GC/EI-MS to confirm individual peak identities of representative
619 replicates. This included the comparison of retention times with authentic
620 standards and by comparison of mass spectra with Wiley, National Institute of
621 Standards and Technology and the Adams libraries.

622 To ensure maximal independence of the second GWAS replicate that was
623 grown in the field, analytical conditions utilized LC-MS instead of GC-MS.

624 Reacted stem tissues were first ground to a fine powder with liquid N₂ and
625 weighed out in 50 mg aliquots. Tissue samples were sequentially and additively
626 bead homogenized in 1) 100 µl 1-propanol: acetonitrile: formic acid (1:1:0.01), 2)
627 250 µl acetonitrile: ethyl acetate (1:1), and 3) 100 µl of H₂O. Each combined
628 sample consisted of a co-miscible acidified solvent mixture of primarily 1-
629 propanol: acetonitrile: ethyl acetate: water in the approximate proportion of
630 11:39:28:22 which was then centrifuged at 15,000 rpm for 20 min. Approximately
631 150 µl the particulate free supernatant was carefully removed for LC/MS
632 automated sample analyses utilizing 5 µl injections. The LC consisted of an
633 Agilent 1260 Infinity series HiP Degasser (G4225A), 1260 binary pump
634 (G1312B), and a 1260 autosampler (G1329B). The binary gradient mobile phase
635 consisted of 0.1% formic acid in H₂O (solvent A) and 0.1% formic acid in MeOH
636 (solvent B). Analytical samples were chromatographically separated on a Zorbax
637 Eclipse Plus C18 Rapid Resolution HD column (Agilent: 1.8 µm, 2.1 x 50 mm)
638 using a 0.35 ml min⁻¹ flow rate. The mobile phase gradient was: 0–2 min, 5% B
639 constant ratio; 3 min, 24% B; 18 min, 98% B, 25 min, 98% B, and 26 min 5% B
640 for column re-equilibration before the next injection. Eluted analytes underwent
641 electrospray ionization (ESI) via an Agilent Jet Stream Source with thermal
642 gradient focusing using the following parameters: nozzle voltage (500 V), N₂
643 nebulizing gas (flow 12 l min⁻¹, 55 psi, 225°C) and sheath gas (350°C, 12 l min⁻¹).
644 The transfer inlet capillary was 3500V and both MS1 and MS2 heaters were at
645 100°C. Negative ionization [M-H]⁻ mode scans (0.1 amu steps, 2.25 cycles s⁻¹)
646 from *m/z* 100 to 1000 were acquired. After considerable unsuccessful attempts to

647 optimize parameters required to obtain meaningful daughter ion fragments from
648 β -costic acid, analyses relied exclusively on the native parent [M-H]⁻ ion m/z 233
649 and stable retention time of 16.65 min separated from established maize
650 zealexins. Quantification utilized an external standard curve of β -costic acid (Ark
651 Pharm, #AK168379, Libertyville, IL, USA) analyzed under identical conditions.

652

653 **Controlled Maize Elicitation Assays**

654 Controlled maize elicitation assays used 30-40 day old greenhouse plants grown
655 in 1-l plastic pots or in the case of the Goodman diversity panel (second
656 replicate) field grown plants. Plants in damage-related treatment groups were slit
657 in the center, spanning both sides of the stem, with a surgical scalpel that was
658 pulled 8–10 cm upward to create a parallel longitudinal incision. The treatment
659 spanned the upper nodes, internodes, and the most basal portion of unexpanded
660 leaves. All fungal spore inoculations (1×10^7 ml⁻¹) treatments were performed in
661 100 μ l of H₂O. For experiments involving stem elicitation with heat-killed
662 *Fusarium* hyphae, crude material was homogenized in a Waring blender at
663 maximum speed for 3 min in the presence of additional H₂O at 20-30% (WT/WT)
664 to create a thick smooth paste. Approximately 500 μ l of crude elicitor was
665 introduced into each slit stem followed by sealing the site with clear plastic
666 packing tape to minimize desiccation of the treated stem tissues. For each
667 individual experiment details relating to specific tissues, biological replications
668 and harvest time points are noted in the figures and captions.

669 For the assay of plant responses to long-term western corn rootworm
670 (WCR; *Diabrotica virgifera virgifera*) herbivory, seeds of an IBM line carrying a
671 functional *ZmTps21* gene (IBM-RIL-0287) were grown in 946 ml DM32R cups
672 (Dart Container Corporation, Mason, MI, USA) filled with greenhouse potting
673 media and fertilized following Gassmann et al. (Gassmann et al., 2011). Seeds
674 were planted 1 month prior to WCR inoculation and maintained at 23°C – 28°C in
675 a greenhouse with supplemental daylight balanced illumination on a 16:8 (L:D)
676 photoperiod. Plants were watered daily as needed to prevent saturated soil
677 conditions. Inoculation and care of \geq V5-V6 stage (Abendroth, 2011) treated
678 plants followed from Gassmann et al. (Gassmann et al., 2011). Cups were
679 inoculated with n=10 neonate WCR larvae (obtained from USDA-ARS-NCARL;
680 Brookings, SD, USA) and held in an incubator at 24°C with 40%-60% RH and
681 watered sparingly as needed to minimize pot flooding. The experiment utilized 4
682 replicates per treatment. After 17 d, 1 g samples of insect attacked and healthy
683 root tissues were collected from the plants, frozen on dry ice and stored for
684 chemical analyses.

685

686 ***Diabrotica* Species Preference and Performance Assays**

687 For studies on preference and performance, WCR eggs and *Diabrotica*
688 *balteata* (LeConte) eggs were obtained from USDA-ARS-NCARL (Brookings,
689 SD, USA) and Syngenta (Syngenta Crop Protection AG, CHE), respectively. All
690 larvae were reared on the roots of germinating maize seedlings until use. For
691 both *Diabrotica* species, 3rd instar larvae were used for all experiments. The

692 performance of *D. virgifera* and *D. balteata* larvae was evaluated by placing one
693 pre-weighed larva into individual solo cups (Bioserv, Newark, DE, USA)
694 containing moist filter paper and a 60 mg crown root section from the B73 inbred.
695 Crown roots were covered with 50 μL β -costic acid in EtOH: H₂O (15 %: 85 %) to
696 create a final tissue concentration of 100 $\mu\text{g g}^{-1}$ FW. Control roots were similarly
697 treated with 50 μL EtOH: H₂O (15 %: 85 %). Larval growth was determined after
698 48 h. The preference of the root herbivores given a choice between control and
699 β -costic acid complemented roots was evaluated in 9 cm dia. petri dishes
700 (Greiner Bio-One GmbH, Frickenhausen, DE). Root tissue treatments followed
701 from the performance experiment. One root of each treatment was placed in the
702 petri dishes. Five larvae were introduced in between the two root sections and
703 larvae feeding behavior was recorded at 0.5, 1, 2, 3 and 4 h after start of the
704 trials.

705

706 **RNA Isolation and qRT-PCR**

707 Total RNA was isolated with TRIzol (Invitrogen, Waltham, MA, USA) according to
708 the manufacturer's protocol. First-strand cDNA was synthesized with the
709 RETROscript reverse transcriptase kit (Ambion, Waltham, MA, USA) using
710 random decamer primers. qRT-PCR was performed using Power SYBR Green
711 Master mix (Applied Biosystems, Waltham, MA, USA), and 250 nM primers on a
712 Bio-Rad CFX96TM Real-Time PCR Detection System. Mean cycle threshold
713 values of triplicate reactions were normalized to EF-1 α (GenBank accession no.
714 AF136829) (Huffaker et al., 2011). Fold-change calculations were performed

715 using the equation $2^{-\Delta\Delta Ct}$ (Livak and Schmittgen, 2001). qRT-PCR primers used
716 in the current study are listed (Supplemental Table S1)

717
718 **Isolation of *ZmTps21* cDNA from Mo17**

719
720 Total RNA was isolated as described above and subjected to TURBO™ DNA-
721 free™ treatment (Ambion) followed by total RNA purification with RNeasy® Mini
722 protocol for RNA cleanup (Qiagen, Hilden, GR). Approximately 1 µg of an equally
723 mixed RNA pool from Mo17 meristem tissues elicited with heat killed *Fusarium*
724 hyphae collected at different time points (8, 24, 32, and 48 h) was used for the
725 construction of 5'- or 3'-RACE cDNA library with SMARTer RACE 5'/3' Kit
726 (Clontech, Mountain View, CA, USA) in accordance with the manufacturers'
727 protocol. The 5'-end of B73-*Zmtps21* was used to design primers for PCR
728 amplification of the Mo17 *ZmTps21* gDNA. A DNA fragment, which was larger
729 than the one from B73 on the agarose gel, was amplified using primers 5'-
730 TGTGAACCAACAAAGCAAGGC-3' and 5'-GAGCTCACCAATCATAGCCTC-3'
731 cloned and sequenced. Based on the conserved sequences between B73 and
732 Mo17, primers were designed to amplify of the 3' and 5' ends *via rapid*
733 amplification of cDNA ends (RACE) (Clontech) from 5'/3' cDNA libraries of
734 *Fusarium* elicited meristems of Mo17. The complete cDNA sequence of the
735 Mo17 functional *ZmTps21* was amplified with the primers Mo17 *ZmTPS21F* (5'-
736 ATGGATGGTGATATTGCTGCCG-3') and Mo17 *ZmTps21R* (5'-
737 TCAGGCACACGGCTTGAGG-3') from the Mo17 5'-RACE cDNA library. Primers
738 used to amplify *ZmTps21* genomic DNA from B73, W22, CML247 and other
739 diverse inbred lines (Ki3, M37W, MS71, M162W, Ki11, Mo18W, HP301, TX303,

740 OH43, Oh7B, KY21, Mo17) are listed (Supplemental Table S1). Corresponding
741 unpublished sequences were deposited in GenBank with following accession
742 numbers (MF614104, MF614105, MF614106, MF614107, MF614108,
743 MF614109, MF614110, MF614111, MF614112, MF614113, MF614114,
744 MF614115).

745

746 **Assay for Terpene Synthase Activity**

747 The complete open reading frame of Mo17 *ZmTps21* was amplified with the
748 primers Mo17 *ZmTps21*-fwd (CACCATGGATGGTGATATTGCTGCCG) and
749 Mo17 *ZmTps21*-rev (TCAGGCACACGGCTTGAGGAAC) and the resulting PCR
750 fragment was cloned into the vector pET100/D-TOPO[®] (Invitrogen, Carlsbad,
751 CA, USA). Sequencing of several clones revealed intact Mo17 *ZmTps21* and two
752 cloning artifacts with altered 3' ends. For heterologous expression in *E. coli*, the
753 plasmids were introduced into the strain BL21 Codon Plus (Invitrogen, Carlsbad,
754 CA, USA). Expression was induced by addition of isopropyl-1-thio-D-
755 galactopyranoside to a final concentration of 1 mM. The cells were collected by
756 centrifugation at 4,000g for 6 min, and disrupted by a 4 × 30 sec treatment with a
757 sonicator in chilled extraction buffer (50 mM MOPS, pH 7.0, with 5 mM MgCl₂, 5
758 mM sodium ascorbate, 0.5 mM PMSF, 5 mM dithiothreitol and 10% v/v glycerol).
759 The cell fragments were removed by centrifugation at 14,000 g, and the
760 supernatant was desalted into assay buffer (10 mM MOPS, pH 7.0, 1 mM
761 dithiothreitol, 10% v/v glycerol) by passage through a Econopac 10DG column
762 (BioRad, Hercules, CA, USA). Enzyme assays were performed in a Teflon[®]-

763 sealed, screw-capped 1 ml GC glass vial containing 50 μ l of the bacterial extract
764 and 50 μ l assay buffer with 10 μ M (*E,E*)-FPP and 10 mM MgCl₂. SPME fiber
765 sample enrichment of adsorbed reaction products and analyses by GC/MS is
766 detailed above in “Identification and Quantification of Metabolites”.

767

768 **Bioassays of *in vitro* and *in vivo* β -costic acid activity as an antifungal**
769 **agent**

770 Maize antifungal assays using purified β -costic acid (Ark Pharm, #AK168379)
771 were performed using the Clinical and Laboratory Standards Institute M38-A2
772 guidelines as previously detailed (Schmelz et al., 2011). In brief, a 96-well
773 microtiter plate-based method using a Synergy4 (BioTech Instruments, Inc.)
774 reader was used to monitor fungal growth at 30 °C in broth media through
775 periodic measurements of changes in OD at 600 nm. Each well contained 200 μ l
776 of initial fungal inoculum (2.5×10^4 conidia ml⁻¹) with 0.5 μ l of either pure DMSO
777 or DMSO containing dilutions of β -costic acid.

778

779 For the mature root infection assays with *Fusarium* pathogens, individual
780 maize plants were greenhouse grown in separate 10-liter pots and supplemented
781 with 14-14-14 Osmocote (Scotts Miracle-Gro) fertilizer. In effort to closely parallel
782 our observations from mature field roots and minimize the invasiveness of
783 belowground treatments, we limited our selection to large nodal roots (≥ 2 mm
784 dia.) containing 1st order lateral roots that were visually apparent and easily
785 accessed following the temporary removal of the pot. Spanning a length of 8 cm,

786 at 1 cm intervals selected nodal roots were punctured with a blunt ended circular
787 steel pin (0.6mm dia) creating a total of 9 punctures. Divided across the 9 wound
788 sites per nodal root and depending on treatment, 100 μ ls of either H₂O or 1×10^7
789 conida mL⁻¹ of either *F. verticillioides* (*F.v.*) or *F. graminearum* (*F.g.*) were
790 applied. Treatments were limited to exposed roots growing along the outer-edge
791 of the soil in close contact with the vertical wall of the plastic pot. Following
792 treatments, plants were carefully placed back into the pots for 7 days. For each
793 line grown, namely B73, m050, Mo17 and m065, 3 treatments and 4 replicates
794 were performed ($4 \times 4 \times 3 = 48$ plants). For determination of the fungal biomass,
795 inoculated and damaged roots were collected 7 days after fungal inoculation.
796 Total genomic DNA was extracted from the infected roots and subjected to real
797 time qPCR using the *F. graminearum*-specific primers for a deoxynivalenol
798 mycotoxin biosynthetic gene (*FgTri6*) and *F. verticillioides* specific primers for a
799 calmodulin (*FvVER1*) gene (Mule et al., 2004; Horevaj et al., 2011) (*SI Appendix*,
800 Table S1). The amount of pathogen DNA relative to plant DNA was estimated by
801 qRT-PCR. Plant DNA quantification utilized a conserved genomic sequence of
802 *ZmTps21/Zmtps21* DNA shared between B73 and Mo17 using forward (gTps21-
803 F, GCAGATGTGTTTCGACAAGTTCC) and reverse (gTps21 R-
804 TTACCTGCAGATTTCTCTAAGCTCTC) primers with calculated amplification
805 efficiencies of 102.65-102.89% between inbreds (Supplemental Table S1).
806 Relative amounts of fungal DNA were calculated by the $2^{-\Delta\Delta C_t}$ method,
807 normalized to a conserved genomic sequence of *ZmTps21/Zmtps21* DNA shared
808 between B73 and Mo17.

809

810 **Statistical Analyses**

811 ANOVAs were performed on the quantified levels of terpenoids, qRT-PCR
812 transcripts, fungal growth and levels of fungal DNA. Treatment effects were
813 investigated when the main effects of the ANOVAs were significant ($P < 0.05$).
814 Tukey tests were used to correct for multiple comparisons between control and
815 treatment groups. The short-term preference and 2-d performance of *Diabrotica*
816 larvae on roots, with and without additional β -costic acid, were analyzed with one
817 sample t-tests and two-way ANOVA using SigmaPlot 13.0 (Systat Software Inc,
818 San Jose, CA, USA), respectively.

819

820 **Supplemental Materials**

821 **Figure S1.** α/β -selinene derived oxidative products, β -costol, β -costal, α -costic
822 acid and β -costic acid coexist as a network of maize metabolites.

823 **Figure S2.** Replicated and comparative association analyses confirm detection
824 of *ZmTps21* as a gene candidate involved in β -costic acid biosynthesis.

825 **Figure S3.** Confirmation of the locus identified by combined linkage and
826 association mapping based on β -costic acid levels using B73 and Mo17 near
827 isogenic lines (NILs).

828 **Figure S4.** Sequence comparison of Mo17 *ZmTps21* with other plant terpene
829 synthases known to catalyze the protonation of neutral reaction intermediates.

830 **Fig. S5.** *ZmTps21* gene structure and sequence polymorphisms across
831 numerous diverse inbred lines support the occurrence of a common and
832 conserved B73-like mutation.

833 **Figure S6.** Deduced amino acid sequence comparison of ZmTps21 across select
834 maize inbred lines.

835 **Figure. S7.** C-terminal modifications in Mo17 ZmTps21 support an influential role
836 in the protonation of germacrene A as putative reaction intermediate

837 **Figure S8.** Germacrene A is minor yet detectable product of Mo17
838 ZmTps21 and is converted to β -elemene during GC injection at 240°C.

839 **Figure S9.** ZmTps21 derived products inhibit fungal growth at
840 physiologically relevant concentrations *in vitro* and can be assessed *in vivo*
841 using IBM near isogenic lines (NILs).

842 **Table S1.** Primers used for qRT-PCR analysis and sequencing *ZmTps21*
843 genomic DNA

844 **Table S2.** Maize lines specifically used to identify *ZmTps21*

845

846

847 **ACKNOWLEDGMENTS**

848 Authors thank Dr. A. Steinbrenner, Dr. K. Dressano, J. Chan, E. Poretsky, A.
849 Sher, K. O'Leary, M. Broemmer, H. Riggelman, S.A. Reyes, and S. Delgado for
850 help in planting, treatments and sampling. N. Rauch (MPICE), T. Vassor (U. of
851 Bern) and M. Petit-Prost (U. of Bern) are thanked for expert technical support. Dr.
852 L. Smith is thanked for shared UCSD Biology Field Station management. With
853 the support of Y. Yoshikuni, this research, or a portion thereof, was performed
854 under the JGI-EMSL Collaborative Science Initiative and used resources at the
855 DOE Joint Genome Institute and the Environmental Molecular Sciences
856 Laboratory, which are DOE Office of Science User Facilities. Both facilities are
857 sponsored by the Office of Biological and Environmental Research and operated
858 under Contract Nos. DE-AC02-05CH11231 (JGI) and DE-AC05-76RL01830

859 (EMSL). Collectively, JGI-EMSL enabled the DOE Joint Genome Institute
860 Community Science Program award (grant #WIP 2568) to E.A.S and A.H.
861 Portions of the research were funded by the NSF-IOS Competitive Award
862 1139329, with primary support from University of California, San Diego startup
863 funds allocated to E.A.S. and A.H.

864 **Figure Legends**

865

866 **Figure 1. β -selinene and β -costic acid can occur as major components of**
867 **maize roots in field grown plants.** Visibly (A) infected or (B) healthy field
868 collected sweet corn (var. Golden Queen) root samples following
869 trimethylsilyldiazomethane derivatization of carboxylic acids to corresponding
870 methyl esters. Labeled peaks in representative GC/EI-MS total ion
871 chromatograms (TIC) include: 1, β -selinene; 2, α -selinene (shoulder); 3, β -costic
872 acid; 4, zealexin A1; and 5, zealexin B1. The presence of common fatty acids,
873 namely palmitic acid and steric acid, are unchanged in healthy root tissues and
874 directly labeled for reference. Corresponding EI spectra (m/z) of (C) β -selinene,
875 (D) α -selinene, and (E) β -costic acid methyl ester from maize field collected
876 roots. (F) Proposed α/β -costic acid biosynthetic pathway in maize starting from
877 farnesyl diphosphate (FPP).

878

879 **Figure 2. β -selinene can exist as a dominant elicited volatile and the**
880 **pathway product β -costic acid can reduce herbivore performance.**
881 Representative GC-FID traces of volatile emissions collected from live roots of
882 field grown maize lines (A) B73, (B) Mo17 and (C) IBM-RIL 0287 20 days after
883 pollination. (D) Average ($n = 4$, \pm SEM) quantity ($\mu\text{g } 12 \text{ h}^{-1} \text{ g}^{-1} \text{ DW}$) of β -selinene
884 volatiles emitted from respective maize roots. Representative GC-FID traces of
885 emitted volatiles collected from living (E) control B73, (F) *C. heterostrophus*-
886 infected B73, (G) control Mo17 and (H) Mo17 *C. heterostrophus*-infected stems.
887 (I) Average ($n = 4$, \pm SEM) quantity ($\text{ng cm}^{-2} \text{ h}^{-1}$) of β -selinene emitted as a
888 volatile from the stems of 5-week-old plants following damage and treatment with
889 H_2O (Dam) or with $100 \mu\text{l}$ of 1×10^7 spores *C. heterostrophus* (*C.h.*). Within plots
890 D and I, different letters (a–c) represent significant differences (All ANOVA P s <
891 0.05; Tukey test corrections for multiple comparisons: $P < 0.05$). (J) Average ($n =$
892 4, \pm SEM) root tissue concentrations ($\mu\text{g g}^{-1} \text{ FW}$) of β -selinene and β -costic acid
893 levels in the roots of IBM-RIL-0287 following 17 days of either no treatment (Ctr)
894 or herbivory by western corn rootworm (WCR) (*Diabrotica virgifera virgifera*)
895 larvae (Student's t-test; one-tailed distribution, equal variance). (K) Average
896 WCR ($n = 18$, \pm SEM) and *Diabrotica balteata* ($n = 57$, \pm SEM) preference over 4
897 h for excised maize roots treated with either EtOH: H_2O (15:85) alone (Control) or
898 the same solution containing β -costic acid to achieve a root tissue concentration
899 of $100 \mu\text{g g}^{-1} \text{ FW}$. Each replicate (n) consisted of assays with 5 individual 3rd
900 instar larvae where distributions were measured at 30,60, 90, 120, 180, 240 min
901 and collectively averaged (one sample t-test, P s > 0.05). (L) Average ($n \geq 5$, \pm
902 SEM) performance (% relative weight gain) of 3rd instar WCR and *D. balteata*
903 larvae over 2 days of feeding on root tissues with (+) and without (-) additions of
904 β -costic acid as described in the preference study (two-way ANOVA $P < 0.05$).

905

906 **Figure 3. Combined linkage and association mapping identifies *ZmTps21***
907 **as a candidate β -selinene synthase.** (A) Major mQTL for β -costic acid
908 production detected on chromosome 9 by composite interval mapping (CIM)
909 using IBM recombinant inbred lines (RILs). (A-insert) Comparative association
910 analysis of the IBM-RIL β -costic acid levels using the General Linear Model
911 (GLM) and 173,984 SNPs. The most statistically significant SNP is located at
912 127,854,265 on Chromosome 9 (B73 RefGen_v2) with a dashed line denoting
913 the 5% Bonferroni correction. (B) Quantile-quantile plot for association analysis
914 of β -costic acid levels in the Goodman diversity panel. (C) Manhattan plot of the
915 association analysis (MLM) of β -costic acid levels in replicate 1 of the Goodman
916 diversity panel following 3 days of fungal elicitation. Dashed line denotes the 5%
917 bonferroni-corrected threshold for 246,477 SNP markers with the most
918 statistically significant SNP located at 127,858,963 (B73 RefGen_v2) on
919 Chromosome 9. (D) Location of the candidate gene *ZmTps21* on the physical
920 map supported by both linkage analysis and association analysis. (E) Fine-
921 mapping with IBM near-isogenic lines (NILs); B73 and Mo17 chromosomal
922 segments are represented by blue and red, respectively. β -costic acid
923 chemotypes of IBM-NILs are indicated as GC/EI-MS traces ($m/z = 233$). (F)
924 Agarose gel PCR amplified products demonstrate a cDNA length polymorphism
925 between B73 *Zmtps21* and Mo17 *ZmTps21* candidates. (G) Diagrammatic
926 structures of B73 *Zmtps21* and Mo17 *ZmTps21* genes based on sequencing.
927 Exons and introns are denoted as rectangular bars and as black lines,
928 respectively. Open rectangle indicates the missing B73 genomic DNA and
929 relative position of encoded conserved RXR and DDXXD motifs terpene cyclase
930 activity.

931

932

933 **Figure 4. Mo17 *ZmTps21* encodes a functional β -selinene synthase.** (A)
934 Mo17 *ZmTps21* was in *Escherichia coli* and the resulting protein extract was
935 incubated with (*E,E*)-farnesyl diphosphate (FPP). Mo17 *ZmTps21* products were
936 collected using solid-phase microextraction and analyzed by GC/MS revealing
937 (2) β -selinene as the dominant product with lower yet detectable levels of (1) β -
938 elemene (germacrene A rearrangement product) and (3) α -selinene. (B) Celery
939 fruit essential oil was used as a natural product standard for β -selinene/ α -
940 selinene (9:1).

941

942

943

944

945

946

947 **Figure 5. *ZmTps21* transcripts are elicited by diverse fungi and precede β -**
948 **costic acid accumulation detectable in diverse maize lines.** Average ($n = 4$;
949 \pm SEM) Mo17 (A) *ZmTps21* (B) β -costic acid (C), *ZmTps6/11* and (D) zealexin A1
950 as qRT-PCR fold changes of transcripts and corresponding phytoalexin
951 concentrations ($\mu\text{g g}^{-1}$ FW) in intact control stems (Con) or those damaged and
952 treated with either H₂O (Dam), or a heat-killed *Fusarium* elicitor (F.E.) hyphae
953 preparation after 1, 2, or 4 days. Average ($n = 4$; \pm SEM) Mo17 (E) *ZmTps21* (F)
954 β -costic acid (G), *ZmTps6/11* and (H) zealexin A1 as qRT-PCR fold changes of
955 transcripts and corresponding phytoalexin concentrations ($\mu\text{g g}^{-1}$ FW) in intact
956 control stems (Con) or those damaged and treated with either 100 μl of H₂O
957 (Dam) alone or spore suspensions ($1 \times 10^7 \text{ ml}^{-1}$) of *R. microsporus* (*R.m.*), *A.*
958 *parasiticus* nor-1 (*A.p.*), *F. verticillioides* (*F.v.*), or *C. heterostrophus* (*C.h.*) and
959 harvested at 2 and 4 days for transcripts and metabolites, respectively. (I)
960 Average ($n = 4$, \pm SEM) β -costic acid concentrations ($\mu\text{g g}^{-1}$ FW) in the scutella of
961 10-d-old maize seedlings from 15 inbred maize lines and mature field collected
962 roots displaying necrosis. Hybrids include sweet corn (var. Golden Queen; GQ)
963 and IBM-RIL0287. Within plots, different letters (a-e) represent significant
964 differences (all ANOVA $P < 0.05$; Tukey test corrections for multiple
965 comparisons: $P < 0.05$).

966

967 **Figure 6. *ZmTps21* derived products inhibit *Fusarium* fungi *in vitro* and**
968 **correspond with improved disease resistance *in vivo*.** Average ($n = 8$, \pm
969 SEM) fungal growth estimates (600 nm OD) of (A) *F. verticillioides*, and (B) *F.*
970 *graminearum*, in liquid media in the presence of β -costic acid at 0 (\circ), 25 (\bullet), and
971 100 (Δ) $\mu\text{g ml}^{-1}$. Average ($n = 4$, \pm SEM) ratio of fungal DNA / plant DNA levels
972 present in maize roots 7 days after damage and inoculation with 100 μl s of either
973 H₂O or 1×10^7 conidia mL^{-1} of (C) *F. verticillioides* and (D) *F. graminearum* in
974 B73, Mo17 and IBM-NILs harboring active (+; m065) and inactive (-; m050)
975 alleles of *ZmTps21*. Within plots, different letters (a–c) represent significant
976 differences (All ANOVA $P < 0.05$; Tukey test corrections for multiple
977 comparisons: $P < 0.05$).

978

979

980

981

982 **LITERATURE CITED**

- 983 **Abendroth LJE, R.W.; Boyer, M.J.; Morley, S.K.** (2011) Corn growth and development. PMR
984 1009 Iowa State University Extension, Ames, Iowa.
- 985 **Ahmad S, Veyrat N, Gordon-Weeks R, Zhang YH, Martin J, Smart L, Glauser G, Erb M, Flors V,**
986 **Frey M, Ton J** (2011) Benzoxazinoid Metabolites Regulate Innate Immunity against
987 Aphids and Fungi in Maize. *Plant Physiol* **157**: 317-327
- 988 **Ahuja I, Kissen R, Bones AM** (2012) Phytoalexins in defense against pathogens. *Trends Plant Sci*
989 **17**: 73-90
- 990 **Ali JG, Alborn HT, Stelinski LL** (2011) Constitutive and induced subterranean plant volatiles
991 attract both entomopathogenic and plant parasitic nematodes. *J Ecol* **99**: 26-35
- 992 **Baldwin IT** (2012) Training a New Generation of Biologists: The Genome-Enabled Field
993 Biologists. *Proc Am Phil Soc* **156**: 205-214
- 994 **Balmer D, de Papajewski DV, Planchamp C, Glauser G, Mauch-Mani B** (2013) Induced
995 resistance in maize is based on organ-specific defence responses. *Plant J* **74**: 213-225
- 996 **Baumgarten AM, Suresh J, May G, Phillips RL** (2007) Mapping QTLs contributing to *Ustilago*
997 *maydis* resistance in specific plant tissues of maize. *Theor. Appl. Genet.* **114**: 1229-1238
- 998 **Beck SD, Kaske ET, Smissman EE** (1957) Resistance factor determination - Quantitative
999 estimation of the resistance factor, 6-methoxybenzoxazolinone, in corn plant tissue. *J*
1000 *Agric Food Chem* **5**: 933-935
- 1001 **Becker EM, Herrfurth C, Irmisch S, Kollner TG, Feussner I, Karlovsky P, Splivallo R** (2014)
1002 Infection of Corn Ears by *Fusarium* spp. Induces the Emission of Volatile Sesquiterpenes.
1003 *J Agric Food Chem* **62**: 5226-5236
- 1004 **Belingheri L, Cartayrade A, Pauly G, Gleizes M** (1992) Partial-purification and properties of the
1005 sesquiterpene beta-selinene cyclase from *Citrofortunella-mitis* fruits. *Plant Sci* **84**: 129-
1006 136
- 1007 **Berger DK, Carstens M, Korsman JN, Middleton F, Kloppers FJ, Tongoona P, Myburg AA** (2014)
1008 Mapping QTL conferring resistance in maize to gray leaf spot disease caused by
1009 *Cercospora zeina*. *BMC Genetics* **15**:60
- 1010 **Borrego E, Kolomiets M** (2016) Synthesis and Functions of Jasmonates in Maize. *Plants* **5**: 41
- 1011 **Bradbury PJ, Zhang Z, Kroon DE, Casstevens TM, Ramdoss Y, Buckler ES** (2007) TASSEL:
1012 software for association mapping of complex traits in diverse samples. *Bioinformatics*
1013 **23**: 2633-2635
- 1014 **Cane DE** (1990) Enzymatic formation of sesquiterpenes. *Chem Rev* **90**: 1089-1103
- 1015 **Casas MI, Falcone-Ferreira ML, Jiang N, Mejia-Guerra MK, Rodriguez E, Wilson T, Engelmeier J,**
1016 **Casati P, Grotewold E** (2016) Identification and Characterization of Maize salmon silks
1017 Genes Involved in Insecticidal Maysin Biosynthesis. *Plant Cell* **28**: 1297-1309
- 1018 **Chen F, Tholl D, Bohlmann J, Pichersky E** (2011) The family of terpene synthases in plants: a
1019 mid-size family of genes for specialized metabolism that is highly diversified throughout
1020 the kingdom. *Plant J* **66**: 212-229
- 1021 **Christensen SA, Huffaker A, Kaplan F, Sims J, Ziemann S, Doehlemann G, Ji L, Schmitz RJ,**
1022 **Kolomiets MV, Alborn HT, Mori N, Jander G, Ni X, Sartor RC, Byers S, Abdo Z, Schmelz**
1023 **EA** (2015) Maize death acids, 9-lipoxygenase-derived cyclopente(a)nones, display
1024 activity as cytotoxic phytoalexins and transcriptional mediators. *Proc Natl Acad Sci USA*
1025 **112**: 11407-11412

- 1026 **Churchill GA, Doerge RW** (1994) Empirical threshold values for quantitative trait mapping.
1027 *Genetics* **138**: 963-971
- 1028 **Cook JP, McMullen MD, Holland JB, Tian F, Bradbury P, Ross-Ibarra J, Buckler ES, Flint-Garcia**
1029 **SA** (2012) Genetic Architecture of Maize Kernel Composition in the Nested Association
1030 Mapping and Inbred Association Panels. *Plant Physiol* **158**: 824-834
- 1031 **Couture RM, Routley DG, Dunn GM** (1971) Role of cyclic hydroxamic acids in monogenic
1032 resistance of maize to *Helminthosporium turcicum*. *Physiol Plant Path* **1**: 515-521
- 1033 **Dangl JL, Horvath DM, Staskawicz BJ** (2013) Pivoting the Plant Immune System from Dissection
1034 to Deployment. *Science* **341**: 746-751
- 1035 **de Kraker JW, Franssen MCR, de Groot A, Shibata T, Bouwmeester HJ** (2001) Germacrenes
1036 from fresh costus roots. *Phytochem* **58**: 481-487
- 1037 **Degenhardt J** (2009) Indirect Defense Responses to Herbivory in Grasses. *Plant Physiol* **149**: 96-
1038 102
- 1039 **Degenhardt J, Hiltbold I, Kollner TG, Frey M, Gierl A, Gershenzon J, Hibbard BE, Ellersieck MR,**
1040 **Turlings TCJ** (2009) Restoring a maize root signal that attracts insect-killing nematodes
1041 to control a major pest. *Proc Natl Acad Sci USA* **106**: 13213-13218
- 1042 **Degenhardt J, Kollner TG, Gershenzon J** (2009) Monoterpene and sesquiterpene synthases and
1043 the origin of terpene skeletal diversity in plants. *Phytochem* **70**: 1621-1637
- 1044 **Eichten SR, Foerster JM, de Leon N, Kai Y, Yeh CT, Liu SZ, Jeddloh JA, Schnable PS, Kaeppler**
1045 **SM, Springer NM** (2011) B73-Mo17 Near-Isogenic Lines Demonstrate Dispersed
1046 Structural Variation in Maize. *Plant Physiol* **156**: 1679-1690
- 1047 **Elshire RJ, Glaubitz JC, Sun Q, Poland JA, Kawamoto K, Buckler ES, Mitchell SE** (2011) A Robust,
1048 Simple Genotyping-by-Sequencing (GBS) Approach for High Diversity Species. *Plos One*
1049 **6(5)**:e19379
- 1050 **Flint-Garcia SA, Dashiell KE, Prischmann DA, Bohn MO, Hibbard BE** (2009) Conventional
1051 Screening Overlooks Resistance Sources: Rootworm Damage of Diverse Inbred Lines and
1052 Their B73 Hybrids Is Unrelated. *J Eco Ent* **102**: 1317-1324
- 1053 **Flint-Garcia SA, Thuillet AC, Yu JM, Pressoir G, Romero SM, Mitchell SE, Doebley J, Kresovich S,**
1054 **Goodman MM, Buckler ES** (2005) Maize association population: a high-resolution
1055 platform for quantitative trait locus dissection. *Plant J* **44**: 1054-1064
- 1056 **Frey M, Schullehner K, Dick R, Fiesselmann A, Gierl A** (2009) Benzoxazinoid biosynthesis, a
1057 model for evolution of secondary metabolic pathways in plants. *Phytochem* **70**: 1645-
1058 1651
- 1059 **Fu JY, Ren F, Lu X, Mao HJ, Xu MM, Degenhardt J, Peters RJ, Wang Q** (2016) A Tandem Array of
1060 ent-Kaurene Synthases in Maize with Roles in Gibberellin and More Specialized
1061 Metabolism. *Plant Physiol* **170**: 742-751
- 1062 **Gardiner JM, Coe EH, Meliahancock S, Hoisington DA, Chao S** (1993) Development of a core rflp
1063 map in maize using an immortalized-f2 population. *Genetics* **134**: 917-930
- 1064 **Gassmann AJ, Petzold-Maxwell JL, Keweshan RS, Dunbar MW** (2011) Field-Evolved Resistance
1065 to Bt Maize by Western Corn Rootworm. *Plos One* **6(7)**: e22629
- 1066 **Gershenzon J, Dudareva N** (2007) The function of terpene natural products in the natural world.
1067 *Nat Chem Biol* **3**: 408-414
- 1068 **Gershenzon J, Kreis, W.** (1999) Biosynthesis of monoterpenes, sesquiterpenes, diterpenes,
1069 sterols, cardiac glycosides and steroid saponins. Sheffield Academic Press, Sheffield
- 1070 **Gray ME, Sappington TW, Miller NJ, Moeser J, Bohn MO** (2009) Adaptation and Invasiveness of
1071 Western Corn Rootworm: Intensifying Research on a Worsening Pest. *In Ann Rev Ent*,
1072 Vol 54, pp 303-321

- 1073 **Handrick V, Robert CAM, Ahern KR, Zhou SQ, Machado RAR, Maag D, Glauser G, Fernandez-**
1074 **Penny FE, Chandran JN, Rodgers-Melnik E, Schneider B, Buckler ES, Boland W,**
1075 **Gershenson J, Jander G, Erb M, Kollner TG** (2016) Biosynthesis of 8-O-Methylated
1076 Benzoxazinoid Defense Compounds in Maize. *Plant Cell* **28**: 1682-1700
- 1077 **Harborne JB** (1999) The comparative biochemistry of phytoalexin induction in plants. *Biochem*
1078 *Syst and Ecol* **27**: 335-367
- 1079 **Hirsch CN, Foerster JM, Johnson JM, Sekhon RS, Muttoni G, Vaillancourt B, Penagaricano F,**
1080 **Lindquist E, Pedraza MA, Barry K, de Leon N, Kaeppler SM, Buell CR** (2014) Insights into
1081 the Maize Pan-Genome and Pan-Transcriptome. *Plant Cell* **26**: 121-135
- 1082 **Horevaj P, Milus EA, Bluhm BH** (2011) A real-time qPCR assay to quantify *Fusarium*
1083 *graminearum* biomass in wheat kernels. *J Appl Microbiol* **111**: 396-406
- 1084 **Huffaker A, Kaplan F, Vaughan MM, Dafoe NJ, Ni X, Rocca JR, Alborn HT, Teal PEA, Schmelz EA**
1085 (2011) Novel Acidic Sesquiterpenoids Constitute a Dominant Class of Pathogen-Induced
1086 Phytoalexins in Maize. *Plant Physiol* **156**: 2082-2097
- 1087 **Huffaker A, Pearce G, Veyrat N, Erb M, Turlings TCJ, Sartor R, Shen Z, Briggs SP, Vaughan MM,**
1088 **Alborn HT, Teal PEA, Schmelz EA** (2013) Plant elicitor peptides are conserved signals
1089 regulating direct and indirect antiherbivore defense. *Proc Natl Acad Sci USA* **110**: 5707-
1090 5712
- 1091 **Iijima Y, Davidovich-Rikanati R, Fridman E, Gang DR, Bar E, Lewinsohn E, Pichersky E** (2004)
1092 The biochemical and molecular basis for the divergent patterns in the biosynthesis of
1093 terpenes and phenylpropenes in the peltate glands of three cultivars of basil. *Plant*
1094 *Physiol* **136**: 3724-3736
- 1095 **Katerinopoulos EH, Isaakidis D, Sofou K, Spyros A** (2011) Use of costic acid or extracts of
1096 *Dittrichia viscosa* against *Varroa destructor*. In: Google Patents
- 1097 **Kollner TG, Held M, Lenk C, Hiltbold I, Turlings TCJ, Gershenson J, Degenhardt J** (2008) A maize
1098 (E)-beta-caryophyllene synthase implicated in indirect defense responses against
1099 herbivores is not expressed in most American maize varieties. *Plant Cell* **20**: 482-494
- 1100 **Kollner TG, Lenk C, Schnee C, Kopke S, Lindemann P, Gershenson J, Degenhardt J** (2013)
1101 Localization of sesquiterpene formation and emission in maize leaves after herbivore
1102 damage. *BMC Plant Biol* **13**:15
- 1103 **Kollner TG, Schnee C, Gershenson J, Degenhardt J** (2004) The sesquiterpene hydrocarbons of
1104 maize (*Zea mays*) form five groups with distinct developmental and organ-specific
1105 distribution. *Phytochem* **65**: 1895-1902
- 1106 **Kollner TG, Schnee C, Gershenson J, Degenhardt J** (2004) The variability of sesquiterpenes
1107 cultivars is controlled by allelic emitted from two *Zea mays* variation of two terpene
1108 synthase genes encoding stereoselective multiple product enzymes. *Plant Cell* **16**: 1115-
1109 1131
- 1110 **Kollner TG, Schnee C, Li S, Svatos A, Schneider B, Gershenson J, Degenhardt J** (2008)
1111 Protonation of a neutral (S)-beta-bisabolene intermediate is involved in (S)-beta-
1112 macrocarpene formation by the maize sesquiterpene synthases TPS6 and TPS11. *J Biol*
1113 *Chem* **283**: 20779-20788
- 1114 **Lanubile A, Ferrarini A, Maschietto V, Delledonne M, Marocco A, Bellin D** (2014) Functional
1115 genomic analysis of constitutive and inducible defense responses to *Fusarium*
1116 *verticillioides* infection in maize genotypes with contrasting ear rot resistance. *BMC*
1117 *Genomics* **15**:710
- 1118 **Lee M, Sharopova N, Beavis WD, Grant D, Katt M, Blair D, Hallauer A** (2002) Expanding the
1119 genetic map of maize with the intermated B73 x Mo17 (IBM) population. *Plant Mol Biol*
1120 **48**: 453-461

- 1121 **Lipka AE, Tian F, Wang QS, Peiffer J, Li M, Bradbury PJ, Gore MA, Buckler ES, Zhang ZW** (2012)
 1122 GAPIT: genome association and prediction integrated tool. *Bioinformatics* **28**: 2397-2399
- 1123 **Livak KJ, Schmittgen TD** (2001) Analysis of relative gene expression data using real-time
 1124 quantitative PCR and the 2(T)(-Delta Delta C) method. *Methods* **25**: 402-408
- 1125 **McMullen MD, Frey M, Degenhardt J** (2009) Genetics and Biochemistry of Insect Resistance in
 1126 Maize. In JL Bennetzen, SC Hake, eds, *Handbook of Maize: Its Biology*. Springer New
 1127 York, New York, NY, pp 271-289
- 1128 **McMullen MD, Kresovich S, Villeda HS, Bradbury P, Li H, Sun Q, Flint-Garcia S, Thornsberry J,**
 1129 **Acharya C, Bottoms C, Brown P, Browne C, Eller M, Guill K, Harjes C, Kroon D, Lepak N,**
 1130 **Mitchell SE, Peterson B, Pressoir G, Romero S, Rosas MO, Salvo S, Yates H, Hanson M,**
 1131 **Jones E, Smith S, Glaubitz JC, Goodman M, Ware D, Holland JB, Buckler ES** (2009)
 1132 Genetic Properties of the Maize Nested Association Mapping Population. *Science* **325**:
 1133 737-740
- 1134 **Meihls LN, Handrick V, Glauser G, Barbier H, Kaur H, Haribal MM, Lipka AE, Gershenzon J,**
 1135 **Buckler ES, Erb M, Kollner TG, Jander G** (2013) Natural Variation in Maize Aphid
 1136 Resistance Is Associated with 2,4-Dihydroxy-7-Methoxy-1,4-Benzoxazin-3-One Glucoside
 1137 Methyltransferase Activity. *Plant Cell* **25**: 2341-2355
- 1138 **Meinke LJ, Sappington TW, Onstad DW, Guillemaud T, Miller NJ, Judith K, Nora L, Furlan L,**
 1139 **Jozsef K, Ferenc T** (2009) Western corn rootworm (*Diabrotica virgifera virgifera*
 1140 LeConte) population dynamics. *Agric For Entomol* **11**: 29-46
- 1141 **Meyer JDF, Snook ME, Houchins KE, Rector BG, Widstrom NW, McMullen MD** (2007)
 1142 Quantitative trait loci for maysin synthesis in maize (*Zea mays* L.) lines selected for high
 1143 silk maysin content. *Theor Appl Genet* **115**: 119-128
- 1144 **Miller NJ, Guillemaud T, Giordano R, Siegfried BD, Gray ME, Meinke LJ, Sappington TW** (2009)
 1145 Genes, gene flow and adaptation of *Diabrotica virgifera virgifera*. *Agric For Entomol* **11**:
 1146 47-60
- 1147 **Mule G, Susca A, Stea G, Moretti A** (2004) A species-specific PCR assay based on the calmodulin
 1148 partial gene for identification of *Fusarium verticillioides*, *F. proliferatum* and *F.*
 1149 *subglutinans*. *Eur J Plant Path* **110**: 495-502
- 1150 **Nguyen DT, Gopfert JC, Ikezawa N, MacNevin G, Kathiresan M, Conrad J, Spring O, Ro DK**
 1151 (2010) Biochemical Conservation and Evolution of Germacrene A Oxidase in Asteraceae.
 1152 *J Bio Chem* **285**: 16588-16598
- 1153 **Olukolu BA, Tracy WF, Wisser R, De Vries B, Balint-Kurti PJ** (2016) A Genome-Wide Association
 1154 Study for Partial Resistance to Maize Common Rust. *Phytopathology* **106**: 745-751
- 1155 **Rao KV, Alvarez FM** (1981) Antibiotic principle of *Eupatorium capillifolium*. *J Nat Prod* **44**: 252-
 1156 256
- 1157 **Rasmann S, Kollner TG, Degenhardt J, Hiltbold I, Toepfer S, Kuhlmann U, Gershenzon J,**
 1158 **Turlings TCJ** (2005) Recruitment of entomopathogenic nematodes by insect-damaged
 1159 maize roots. *Nature* **434**: 732-737
- 1160 **Richter A, Schaff C, Zhang Z, Lipka AE, Tian F, Köllner TG, Schnee C, Preiß S, Irmisch S, Jander G,**
 1161 **Boland W, Gershenzon J, Buckler ES, Degenhardt J** (2016) Characterization of
 1162 Biosynthetic Pathways for the Production of the Volatile Homoterpenes DMNT and
 1163 TMTT in *Zea mays*. *Plant Cell* **28**: 2651-2665
- 1164 **Saba F** (1970) Host plant spectrum and temperature limitations of *Diabrotica balteata*. *Canad*
 1165 *Entomol* **102**: 684-&
- 1166 **Samayoa LF, Malvar RA, Olukolu BA, Holland JB, Butron A** (2015) Genome-wide association
 1167 study reveals a set of genes associated with resistance to the Mediterranean corn borer
 1168 (*Sesamia nonagrioides* L.) in a maize diversity panel. *BMC Plant Biol* **15**:35

- 1169 **Schmelz EA, Alborn HT, Tumlinson JH** (2001) The influence of intact-plant and excised-leaf
1170 bioassay designs on volicitin- and jasmonic acid-induced sesquiterpene volatile release
1171 in *Zea mays*. *Planta* **214**: 171-179
- 1172 **Schmelz EA, Engelberth J, Alborn HT, Tumlinson JH, Teal PEA** (2009) Phytohormone-based
1173 activity mapping of insect herbivore-produced elicitors. *Proc Natl Acad Sci USA* **106**: 653-
1174 657
- 1175 **Schmelz EA, Engelberth J, Tumlinson JH, Block A, Alborn HT** (2004) The use of vapor phase
1176 extraction in metabolic profiling of phytohormones and other metabolites. *Plant J* **39**:
1177 790-808
- 1178 **Schmelz EA, Huffaker A, Sims JW, Christensen SA, Lu X, Okada K, Peters RJ** (2014) Biosynthesis,
1179 elicitation and roles of monocot terpenoid phytoalexins. *Plant J* **79**: 659-678
- 1180 **Schmelz EA, Kaplan F, Huffaker A, Dafoe NJ, Vaughan MM, Ni X, Rocca JR, Alborn HT, Teal PE**
1181 (2011) Identity, regulation, and activity of inducible diterpenoid phytoalexins in maize.
1182 *Proc Natl Acad Sci USA* **108**: 5455-5460
- 1183 **Schnee C, Kollner TG, Gershenzon J, Degenhardt J** (2002) The maize gene terpene synthase 1
1184 encodes a sesquiterpene synthase catalyzing the formation of (E)-beta-farnesene, (E)-
1185 nerolidol, and (E,E)-farnesol after herbivore damage. *Plant Physiol* **130**: 2049-2060
- 1186 **Schnee C, Kollner TG, Held M, Turlings TCJ, Gershenzon J, Degenhardt J** (2006) The products of
1187 a single maize sesquiterpene synthase form a volatile defense signal that attracts
1188 natural enemies of maize herbivores. *Proc Natl Acad Sci USA* **103**: 1129-1134
- 1189 **Sowbhagya HB** (2014) Chemistry, technology, and nutraceutical functions of celery (*Apium*
1190 *graveolens* L.): an overview. *Crit Rev Food Sci Nutr* **54**: 389-398
- 1191 **Spencer JL, Hibbard BE, Moeser J, Onstad DW** (2009) Behaviour and ecology of the western
1192 corn rootworm (*Diabrotica virgifera virgifera* LeConte). *Agricul For Entomol* **11**: 9-27
- 1193 **Starks CM, Back KW, Chappell J, Noel JP** (1997) Structural basis for cyclic terpene biosynthesis
1194 by tobacco 5-epi-aristolochene synthase. *Science* **277**: 1815-1820
- 1195 **Tinsley NA, Estes RE, Gray ME** (2013) Validation of a nested error component model to estimate
1196 damage caused by corn rootworm larvae. *J Appl Entomol* **137**: 161-169
- 1197 **Turlings TCJ, Tumlinson JH, Lewis WJ** (1990) Exploitation of herbivore-induced plant odors by
1198 host-seeking parasitic wasps. *Science* **250**: 1251-1253
- 1199 **Turner SD** (2014) qqman: an R package for visualizing GWAS results using QQ and Manhattan
1200 plots. Preprint at bioRxiv <http://dx.doi.org/10.1101/005165>
- 1201 **Vanetten HD, Mansfield JW, Bailey JA, Farmer EE** (1994) 2 Classes of plant antibiotics -
1202 phytoalexins versus phytoanticipins. *Plant Cell* **6**: 1191-1192
- 1203 **VanRaden PM** (2008) Efficient Methods to Compute Genomic Predictions. *J Dairy Sci* **91**: 4414-
1204 4423
- 1205 **Vaughan MM, Christensen S, Schmelz EA, Huffaker A, McAuslane HJ, Alborn HT, Romero M,**
1206 **Allen LH, Teal PEA** (2015) Accumulation of terpenoid phytoalexins in maize roots is
1207 associated with drought tolerance. *Plant Cell Environ* **38**: 2195-2207
- 1208 **Wu QX, Shi YP, Jia ZJ** (2006) Eudesmane sesquiterpenoids from the Asteraceae family. *Nat Prod*
1209 *Rep* **23**: 699-734
- 1210 **Yan J, Lipka AE, Schmelz EA, Buckler ES, Jander G** (2015) Accumulation of 5-hydroxynorvaline in
1211 maize (*Zea mays*) leaves is induced by insect feeding and abiotic stress. *J Exp Bot* **66**:
1212 593-602
- 1213 **Yu JM, Pressoir G, Briggs WH, Bi IV, Yamasaki M, Doebley JF, McMullen MD, Gaut BS, Nielsen**
1214 **DM, Holland JB, Kresovich S, Buckler ES** (2006) A unified mixed-model method for
1215 association mapping that accounts for multiple levels of relatedness. *Nat Genet* **38**: 203-
1216 208

1217 **Zhang ZW, Ersoz E, Lai CQ, Todhunter RJ, Tiwari HK, Gore MA, Bradbury PJ, Yu JM, Arnett DK,**
1218 **Ordovas JM, Buckler ES (2010)** Mixed linear model approach adapted for genome-wide
1219 association studies. *Nat Genet* **42**: 355-U118
1220
1221
1222

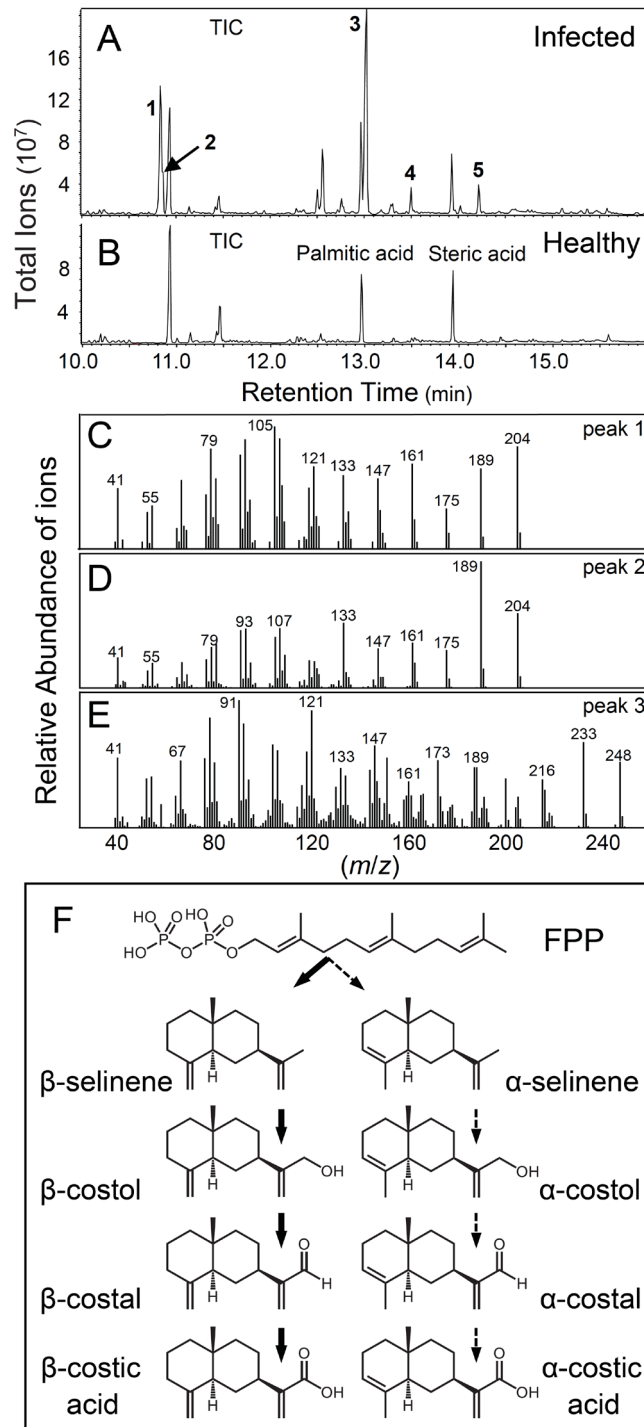


Figure 1. β -selinene and β -costic acid can occur as major components of maize roots in field grown plants. Visibly (A) infected or (B) healthy field collected sweet corn (var. Golden Queen) root samples following trimethylsilyldiazomethane derivatization of carboxylic acids to corresponding methyl esters. Labeled peaks in representative GC/EI-MS total ion chromatograms (TIC) include: 1, β -selinene; 2, α -selinene (shoulder); 3, β -costic acid; 4, zealexin A1; and 5, zealexin B1. The presence of common fatty acids, namely palmitic acid and steric acid, are unchanged in healthy root tissues and directly labeled for reference. Corresponding EI spectra (m/z) of (C) β -selinene, (D) α -selinene, and (E) β -costic acid methyl ester from maize field collected roots. (F) Proposed α/β -costic acid biosynthetic pathway in maize starting from farnesyl diphosphate (FPP).

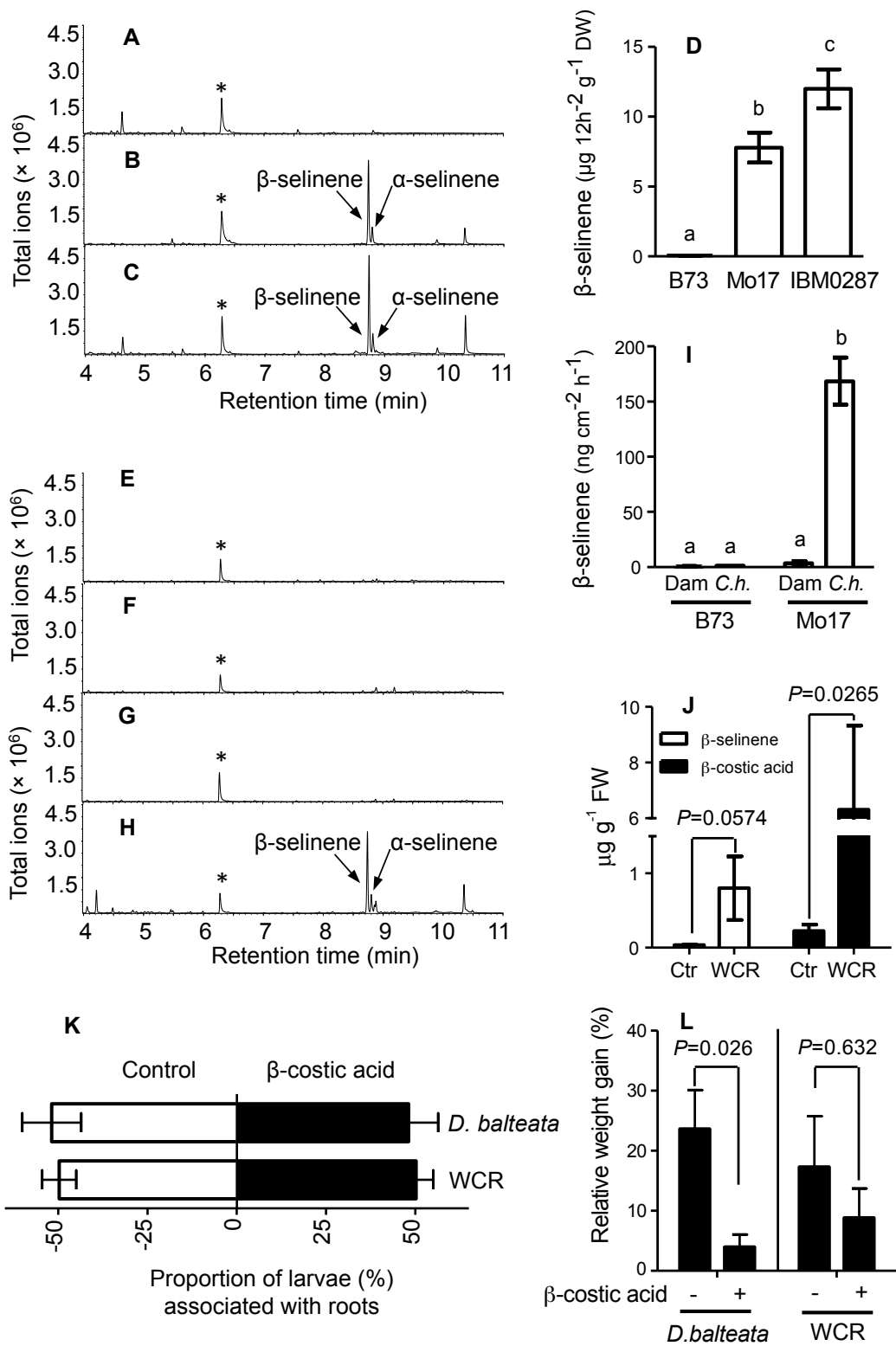


Figure 2. β -selinene can exist as a dominant elicited volatile and the pathway product β -costic acid can reduce herbivore performance. Representative GC-FID traces of volatile emissions collected from live roots of field grown maize lines (A) B73, (B) Mo17 and (C) IBM-RIL 0287 20 days after pollination. (D) Average ($n = 4$, \pm SEM) quantity ($\mu\text{g } 12 \text{ h}^{-1} \text{ g}^{-1} \text{ DW}$) of β -selinene volatiles emitted from respective maize roots. Representative GC-FID traces of emitted volatiles collected from living (E) control B73, (F) *C. heterostrophus*-infected B73, (G) control Mo17 and (H) Mo17 *C. heterostrophus*-infected stems. (I) Average ($n = 4$, \pm SEM) quantity ($\text{ng cm}^{-2} \text{ h}^{-1}$) of β -selinene emitted as a volatile from the stems of 5-week-old plants following damage and treatment with H_2O (Dam) or with $100 \mu\text{l}$ of 1×10^7 spores *C. heterostrophus* (*C.h.*). Within plots D and I, different letters (a–c) represent significant differences (All ANOVA P s < 0.05 ; Tukey test corrections for multiple comparisons: $P < 0.05$). (J) Average ($n = 4$, \pm SEM) root tissue concentrations ($\mu\text{g g}^{-1} \text{ FW}$) of β -selinene and β -costic acid levels in the roots of IBM-RIL-0287 following 17 days of either no treatment (Ctr) or herbivory by western corn rootworm (WCR) (*Diabrotica virgifera virgifera*) larvae (Student's t-test; one-tailed distribution, equal variance). (K) Average WCR ($n = 18$, \pm SEM) and *Diabrotica balteata* ($n = 57$, \pm SEM) preference over 4 h for excised maize roots treated with either EtOH:H₂O (15:85) alone (Control) or the same solution containing β -costic acid to achieve a root tissue concentration of $100 \mu\text{g g}^{-1} \text{ FW}$. Each replicate (n) consisted of assays with 5 individual 3rd instar larvae where distributions were measured at 30, 60, 90, 120, 180, 240 min and collectively averaged (one sample t-test, P s > 0.05). (L) Average ($n \geq 5$, \pm SEM) performance (% relative weight gain) of 3rd instar WCR and *D. balteata* larvae over 2 days of feeding on root tissues with (+) and without (-) additions of β -costic acid as described in the preference study (two-way ANOVA $P < 0.05$).

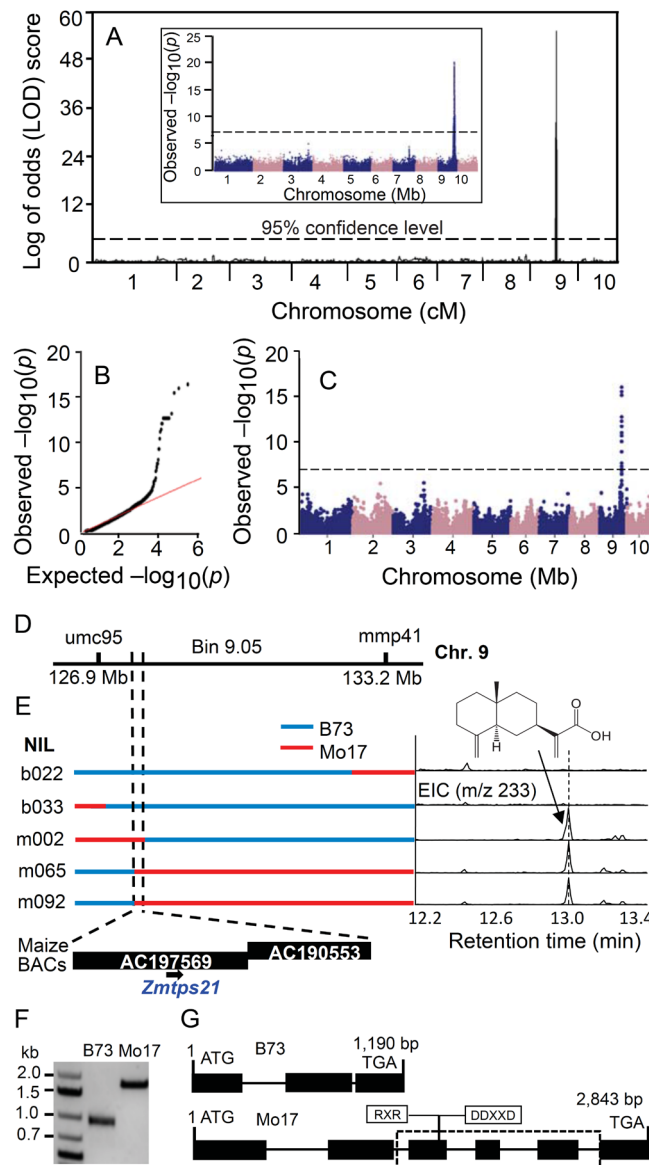


Figure 3. Combined linkage and association mapping identifies *ZmTps21* as a candidate β -selinene synthase. (A) Major mQTL for β -costic acid production detected on chromosome 9 by composite interval mapping (CIM) using IBM recombinant inbred lines (RILs). (A-insert) Comparative association analysis of the IBM-RIL β -costic acid levels using the General Linear Model (GLM) and 173,984 SNPs. The most statistically significant SNP is located at 127,854,265 on Chromosome 9 (B73 RefGen_v2) with a dashed line denoting the 5% Bonferroni correction. (B) Quantile-quantile plot for association analysis of β -costic acid levels in the Goodman diversity panel. (C) Manhattan plot of the association analysis (MLM) of β -costic acid levels in replicate 1 of the Goodman diversity panel following 3 days of fungal elicitation. Dashed line denotes the 5% bonferroni-corrected threshold for 246,477 SNP markers with the most statistically significant SNP located at 127,858,963 (B73 RefGen_v2) on Chromosome 9. (D) Location of the candidate gene *ZmTps21* on the physical map supported by both linkage analysis and association analysis. (E) Fine-mapping with IBM near-isogenic lines (NILs); B73 and Mo17 chromosomal segments are represented by blue and red, respectively. β -costic acid chemotypes of IBM-NILs are indicated as GC/EI-MS traces ($m/z = 233$). (F) Agarose gel PCR amplified products demonstrate a cDNA length polymorphism between B73 *ZmTps21* and Mo17 *ZmTps21* candidates. (G) Diagrammatic structures of B73 *ZmTps21* and Mo17 *ZmTps21* genes based on sequencing. Exons and introns are denoted as rectangular bars and as black lines, respectively. Open rectangle indicates the missing B73 genomic DNA and relative position of encoded conserved RXR and DDXXD domains.

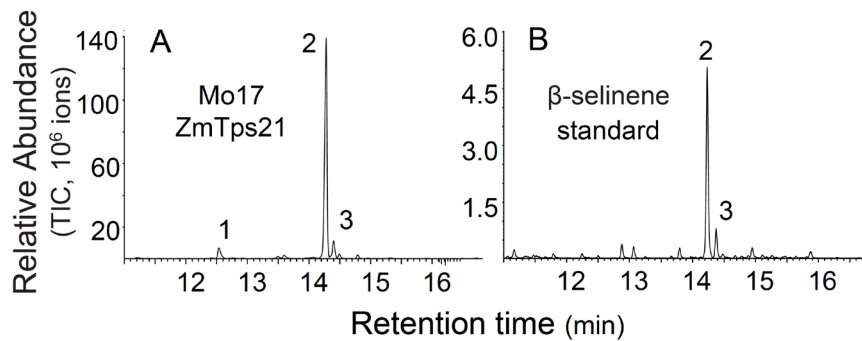


Figure 4. Mo17 *ZmTps21* encodes a functional β -selinene synthase. (A) Mo17 *ZmTps21* was in *Escherichia coli* and the resulting protein extract was incubated with (*E,E*)-farnesyl diphosphate (FPP). Mo17 *ZmTps21* products were collected using solid-phase microextraction and analyzed by GC/MS revealing (2) β -selinene as the dominant product with lower yet detectable levels of (1) β -elemene (germacrene A rearranged product) and (3) α -selinene. (B) Celery fruit essential oil was used as a natural product standard for β -selinene/ α -selinene (9:1).

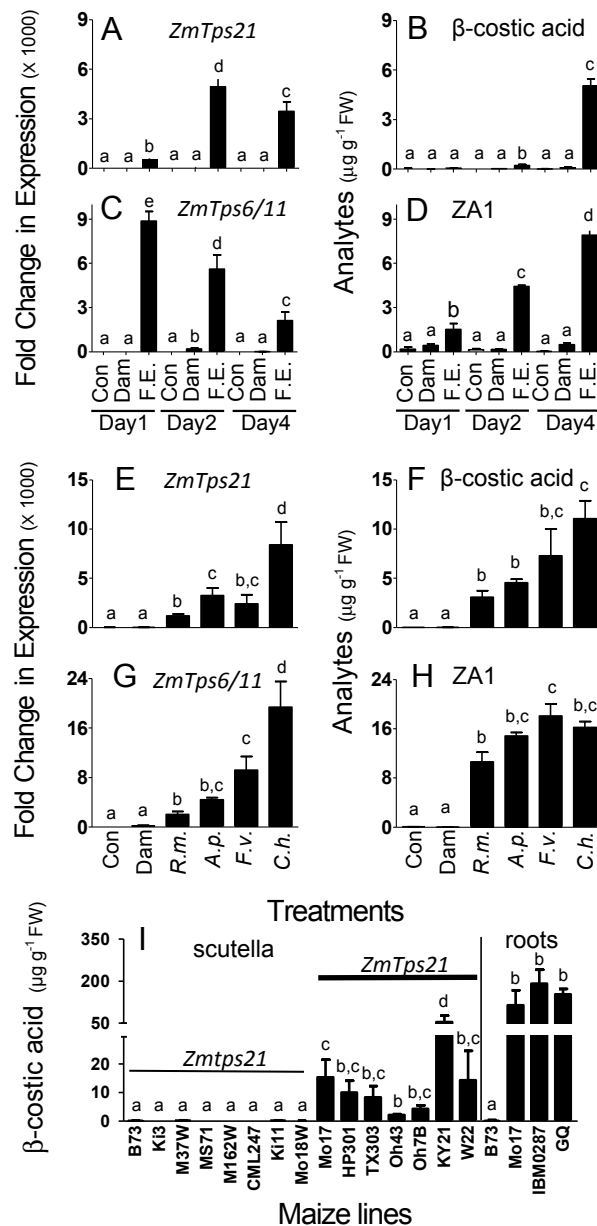


Figure 5. *ZmTps21* transcripts are elicited by diverse fungi and precede β -costic acid accumulation detectable in diverse maize lines. Average ($n = 4$; \pm SEM) Mo17 (A) *ZmTps21* (B) β -costic acid (C), *ZmTps6/11* and (D) zealexin A1 as qRT-PCR fold changes of transcripts and corresponding phytoalexin concentrations ($\mu\text{g g}^{-1}$ FW) in intact control stems (Con) or those damaged and treated with either H_2O (Dam), or a heat-killed *Fusarium* elicitor (F.E.) hyphae preparation after 1, 2, or 4 days. Average ($n = 4$; \pm SEM) Mo17 (E) *ZmTps21* (F) β -costic acid (G), *ZmTps6/11* and (H) zealexin A1 as qRT-PCR fold changes of transcripts and corresponding phytoalexin concentrations ($\mu\text{g g}^{-1}$ FW) in intact control stems (Con) or those damaged and treated with either 100 μl of H_2O (Dam) alone or spore suspensions ($1 \times 10^7 \text{ ml}^{-1}$) of *R. microsporus* (*R.m.*), *A. parasiticus* nor-1 (*A.p.*), *F. verticillioides* (*F.v.*), or *C. heterostrophus* (*C.h.*) and harvested at 2 and 4 days for transcripts and metabolites, respectively. (I) Average ($n = 4$, \pm SEM) β -costic acid concentrations ($\mu\text{g g}^{-1}$ FW) in the scutella of 10-d-old maize seedlings from 15 inbred maize lines and mature field collected roots displaying necrosis. Hybrids include sweet corn (var. Golden Queen; GQ) and IBM-RIL0287. Within plots, different letters (a-e) represent significant differences (all ANOVA $P < 0.05$; Tukey test corrections for multiple comparisons: $P < 0.05$).

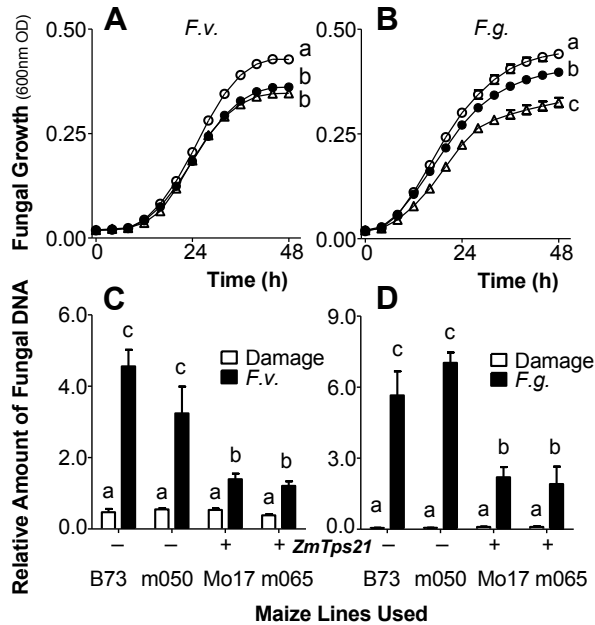


Figure 6. ZmTps21 derived products inhibit *Fusarium* fungi *in vitro* and correspond with improved disease resistance *in vivo*. Average ($n = 8$, \pm SEM) fungal growth estimates (600 nm OD) of (A) *F. verticillioides*, and (B) *F. graminearum*, in liquid media in the presence of β -cotic acid at 0 (\circ), 25 (\bullet), and 100 (Δ) $\mu\text{g ml}^{-1}$. Average ($n = 4$, \pm SEM) ratio of fungal DNA / plant DNA levels present in maize roots 7 days after damage and inoculation with 100 μl of either H_2O or 1×10^7 conida ml^{-1} of (C) *F. verticillioides* and (D) *F. graminearum* in B73, Mo17 and IBM-NILs harboring active (+; m065) and inactive (-; m050) alleles of *ZmTps21*. Within plots, different letters (a–c) represent significant differences (All ANOVA $P < 0.05$; Tukey test corrections for multiple comparisons: $P < 0.05$).

Parsed Citations

Abendroth LJE, R.W.; Boyer, M.J.; Morley, S.K. (2011) Corn growth and development. PMR 1009 Iowa State University Extension, Ames, Iowa.

Pubmed: [Author and Title](#)

CrossRef: [Author and Title](#)

Google Scholar: [Author Only](#) [Title Only](#) [Author and Title](#)

Ahmad S, Veyrat N, Gordon-Weeks R, Zhang YH, Martin J, Smart L, Glauser G, Erb M, Flors V, Frey M, Ton J (2011) Benzoxazinoid Metabolites Regulate Innate Immunity against Aphids and Fungi in Maize. Plant Physiol 157: 317-327

Pubmed: [Author and Title](#)

CrossRef: [Author and Title](#)

Google Scholar: [Author Only](#) [Title Only](#) [Author and Title](#)

Ahuja I, Kissen R, Bones AM (2012) Phytoalexins in defense against pathogens. Trends Plant Sci 17: 73-90

Pubmed: [Author and Title](#)

CrossRef: [Author and Title](#)

Google Scholar: [Author Only](#) [Title Only](#) [Author and Title](#)

Ali JG, Alborn HT, Stelinski LL (2011) Constitutive and induced subterranean plant volatiles attract both entomopathogenic and plant parasitic nematodes. J Ecol 99: 26-35

Pubmed: [Author and Title](#)

CrossRef: [Author and Title](#)

Google Scholar: [Author Only](#) [Title Only](#) [Author and Title](#)

Baldwin IT (2012) Training a New Generation of Biologists: The Genome-Enabled Field Biologists. Proc Am Phil Soc 156: 205-214

Pubmed: [Author and Title](#)

CrossRef: [Author and Title](#)

Google Scholar: [Author Only](#) [Title Only](#) [Author and Title](#)

Balmer D, de Papajewski DV, Planchamp C, Glauser G, Mauch-Mani B (2013) Induced resistance in maize is based on organ-specific defence responses. Plant J 74: 213-225

Pubmed: [Author and Title](#)

CrossRef: [Author and Title](#)

Google Scholar: [Author Only](#) [Title Only](#) [Author and Title](#)

Baumgarten AM, Suresh J, May G, Phillips RL (2007) Mapping QTLs contributing to Ustilago maydis resistance in specific plant tissues of maize. Theor. Appl. Genet. 114: 1229-1238

Pubmed: [Author and Title](#)

CrossRef: [Author and Title](#)

Google Scholar: [Author Only](#) [Title Only](#) [Author and Title](#)

Beck SD, Kaske ET, Smismann EE (1957) Resistance factor determination - Quantitative estimation of the resistance factor, 6-methoxybenzoxazolinone, in corn plant tissue. J Agric Food Chem 5: 933-935

Pubmed: [Author and Title](#)

CrossRef: [Author and Title](#)

Google Scholar: [Author Only](#) [Title Only](#) [Author and Title](#)

Becker EM, Herrfurth C, Irmisch S, Kollner TG, Feussner I, Karlovsky P, Splivallo R (2014) Infection of Corn Ears by Fusarium spp. Induces the Emission of Volatile Sesquiterpenes. J Agric Food Chem 62: 5226-5236

Pubmed: [Author and Title](#)

CrossRef: [Author and Title](#)

Google Scholar: [Author Only](#) [Title Only](#) [Author and Title](#)

Belingheri L, Cartayrade A, Pauly G, Gleizes M (1992) Partial-purification and properties of the sesquiterpene beta-selinene cyclase from Citrofortunella-mitis fruits. Plant Sci 84: 129-136

Pubmed: [Author and Title](#)

CrossRef: [Author and Title](#)

Google Scholar: [Author Only](#) [Title Only](#) [Author and Title](#)

Berger DK, Carstens M, Korsman JN, Middleton F, Kloppers FJ, Tongoona P, Myburg AA (2014) Mapping QTL conferring resistance in maize to gray leaf spot disease caused by Cercospora zeina. BMC Genetics 15:60

Pubmed: [Author and Title](#)

CrossRef: [Author and Title](#)

Google Scholar: [Author Only](#) [Title Only](#) [Author and Title](#)

Borrego E, Kolomiets M (2016) Synthesis and Functions of Jasmonates in Maize. Plants 5: 41

Pubmed: [Author and Title](#)

CrossRef: [Author and Title](#)

Google Scholar: [Author Only](#) [Title Only](#) [Author and Title](#)

Bradbury PJ, Zhang Z, Kroon DE, Casstevens TM, Ramdoss Y, Buckler ES (2007) TASSEL: software for association mapping of complex traits in diverse samples. Bioinformatics 23: 2633-2635

Pubmed: [Author and Title](#)

CrossRef: [Author and Title](#)

Google Scholar: [Author Only](#) [Title Only](#) [Author and Title](#)

Cane DE (1990) Enzymatic formation of sesquiterpenes. Chem Rev 90: 1089-1103

Pubmed: [Author and Title](#)

CrossRef: [Author and Title](#)

Google Scholar: [Author Only](#) [Title Only](#) [Author and Title](#)

Casas MI, Falcone-Ferreira ML, Jiang N, Mejia-Guerra MK, Rodriguez E, Wilson T, Engelmeier J, Casati P, Grotewold E (2016) Identification and Characterization of Maize salmon silks Genes Involved in Insecticidal Maysin Biosynthesis. Plant Cell 28: 1297-1309

Pubmed: [Author and Title](#)

CrossRef: [Author and Title](#)

Google Scholar: [Author Only](#) [Title Only](#) [Author and Title](#)

Chen F, Tholl D, Bohlmann J, Pichersky E (2011) The family of terpene synthases in plants: a mid-size family of genes for specialized metabolism that is highly diversified throughout the kingdom. Plant J 66: 212-229

Pubmed: [Author and Title](#)

CrossRef: [Author and Title](#)

Google Scholar: [Author Only](#) [Title Only](#) [Author and Title](#)

Christensen SA, Huffaker A, Kaplan F, Sims J, Ziemann S, Doehlemann G, Ji L, Schmitz RJ, Kolomiets MV, Alborn HT, Mori N, Jander G, Ni X, Sartor RC, Byers S, Abdo Z, Schmelz EA (2015) Maize death acids, 9-lipoxygenase-derived cyclopentane(a)nones, display activity as cytotoxic phytoalexins and transcriptional mediators. Proc Natl Acad Sci USA 112: 11407-11412

Pubmed: [Author and Title](#)

CrossRef: [Author and Title](#)

Google Scholar: [Author Only](#) [Title Only](#) [Author and Title](#)

Churchill GA, Doerge RW (1994) Empirical threshold values for quantitative trait mapping. Genetics 138: 963-971

Pubmed: [Author and Title](#)

CrossRef: [Author and Title](#)

Google Scholar: [Author Only](#) [Title Only](#) [Author and Title](#)

Cook JP, McMullen MD, Holland JB, Tian F, Bradbury P, Ross-Ibarra J, Buckler ES, Flint-Garcia SA (2012) Genetic Architecture of Maize Kernel Composition in the Nested Association Mapping and Inbred Association Panels. Plant Physiol 158: 824-834

Pubmed: [Author and Title](#)

CrossRef: [Author and Title](#)

Google Scholar: [Author Only](#) [Title Only](#) [Author and Title](#)

Couture RM, Routley DG, Dunn GM (1971) Role of cyclic hydroxamic acids in monogenic resistance of maize to Helminthosporium turcicum. Physiol Plant Path 1: 515-521

Pubmed: [Author and Title](#)

CrossRef: [Author and Title](#)

Google Scholar: [Author Only](#) [Title Only](#) [Author and Title](#)

Dangl JL, Horvath DM, Staskawicz BJ (2013) Pivoting the Plant Immune System from Dissection to Deployment. Science 341: 746-751

Pubmed: [Author and Title](#)

CrossRef: [Author and Title](#)

Google Scholar: [Author Only](#) [Title Only](#) [Author and Title](#)

de Kraker JW, Franssen MCR, de Groot A, Shibata T, Bouwmeester HJ (2001) Germacrenes from fresh costus roots. Phytochem 58: 481-487

Pubmed: [Author and Title](#)

CrossRef: [Author and Title](#)

Google Scholar: [Author Only](#) [Title Only](#) [Author and Title](#)

Degenhardt J (2009) Indirect Defense Responses to Herbivory in Grasses. Plant Physiol 149: 96-102

Pubmed: [Author and Title](#)

CrossRef: [Author and Title](#)

Google Scholar: [Author Only](#) [Title Only](#) [Author and Title](#)

Degenhardt J, Hiltbold I, Kollner TG, Frey M, Gierl A, Gershenzon J, Hibbard BE, Ellersieck MR, Turlings TCJ (2009) Restoring a maize root signal that attracts insect-killing nematodes to control a major pest. Proc Natl Acad Sci USA 106: 13213-13218

Pubmed: [Author and Title](#)

CrossRef: [Author and Title](#)

Google Scholar: [Author Only](#) [Title Only](#) [Author and Title](#)

Degenhardt J, Kollner TG, Gershenzon J (2009) Monoterpene and sesquiterpene synthases and the origin of terpene skeletal diversity in plants. Phytochem 70: 1621-1637

Pubmed: [Author and Title](#)

CrossRef: [Author and Title](#)

Google Scholar: [Author Only](#) [Title Only](#) [Author and Title](#)

Eichten SR, Foerster JM, de Leon N, Kai Y, Yeh CT, Liu SZ, Jeddloh JA, Schnable PS, Kaeppler SM, Springer NM (2011) B73-Mo17 Near-Isogenic Lines Demonstrate Dispersed Structural Variation in Maize. Plant Physiol 156: 1679-1690

Pubmed: [Author and Title](#)

CrossRef: [Author and Title](#)

Google Scholar: [Author Only](#) [Title Only](#) [Author and Title](#)

Elshire RJ, Glaubitz JC, Sun Q, Poland JA, Kawamoto K, Buckler ES, Mitchell SE (2011) A Robust, Simple Genotyping-by-Sequencing (GBS) Approach for High Diversity Species. *Plos One* 6(5):e19379

Pubmed: [Author and Title](#)

CrossRef: [Author and Title](#)

Google Scholar: [Author Only](#) [Title Only](#) [Author and Title](#)

Flint-Garcia SA, Dashiell KE, Prischmann DA, Bohn MO, Hibbard BE (2009) Conventional Screening Overlooks Resistance Sources: Rootworm Damage of Diverse Inbred Lines and Their B73 Hybrids Is Unrelated. *J Eco Ent* 102: 1317-1324

Pubmed: [Author and Title](#)

CrossRef: [Author and Title](#)

Google Scholar: [Author Only](#) [Title Only](#) [Author and Title](#)

Flint-Garcia SA, Thuillet AC, Yu JM, Pressoir G, Romero SM, Mitchell SE, Doebley J, Kresovich S, Goodman MM, Buckler ES (2005) Maize association population: a high-resolution platform for quantitative trait locus dissection. *Plant J* 44: 1054-1064

Pubmed: [Author and Title](#)

CrossRef: [Author and Title](#)

Google Scholar: [Author Only](#) [Title Only](#) [Author and Title](#)

Frey M, Schullehner K, Dick R, Fiesselmann A, Gierl A (2009) Benzoxazinoid biosynthesis, a model for evolution of secondary metabolic pathways in plants. *Phytochem* 70: 1645-1651

Pubmed: [Author and Title](#)

CrossRef: [Author and Title](#)

Google Scholar: [Author Only](#) [Title Only](#) [Author and Title](#)

Fu JY, Ren F, Lu X, Mao HJ, Xu MM, Degenhardt J, Peters RJ, Wang Q (2016) A Tandem Array of ent-Kaurene Synthases in Maize with Roles in Gibberellin and More Specialized Metabolism. *Plant Physiol* 170: 742-751

Pubmed: [Author and Title](#)

CrossRef: [Author and Title](#)

Google Scholar: [Author Only](#) [Title Only](#) [Author and Title](#)

Gardiner JM, Coe EH, Meliahancock S, Hoisington DA, Chao S (1993) Development of a core rflp map in maize using an immortalized-f2 population. *Genetics* 134: 917-930

Pubmed: [Author and Title](#)

CrossRef: [Author and Title](#)

Google Scholar: [Author Only](#) [Title Only](#) [Author and Title](#)

Gassmann AJ, Petzold-Maxwell JL, Keweshan RS, Dunbar MW (2011) Field-Evolved Resistance to Bt Maize by Western Corn Rootworm. *Plos One* 6(7): e22629

Pubmed: [Author and Title](#)

CrossRef: [Author and Title](#)

Google Scholar: [Author Only](#) [Title Only](#) [Author and Title](#)

Gershenzon J, Dudareva N (2007) The function of terpene natural products in the natural world. *Nat Chem Biol* 3: 408-414

Pubmed: [Author and Title](#)

CrossRef: [Author and Title](#)

Google Scholar: [Author Only](#) [Title Only](#) [Author and Title](#)

Gershenzon J, Kreis, W. (1999) Biosynthesis of monoterpenes, sesquiterpenes, diterpenes, sterols, cardiac glycosides and steroid saponins. Sheffield Academic Press, Sheffield

Pubmed: [Author and Title](#)

CrossRef: [Author and Title](#)

Google Scholar: [Author Only](#) [Title Only](#) [Author and Title](#)

Gray ME, Sappington TW, Miller NJ, Moeser J, Bohn MO (2009) Adaptation and Invasiveness of Western Corn Rootworm: Intensifying Research on a Worsening Pest. In *Ann Rev Ent*, Vol 54, pp 303-321

Pubmed: [Author and Title](#)

CrossRef: [Author and Title](#)

Google Scholar: [Author Only](#) [Title Only](#) [Author and Title](#)

Handrick V, Robert CAM, Ahern KR, Zhou SQ, Machado RAR, Maag D, Glauser G, Fernandez-Penny FE, Chandran JN, Rodgers-Melnik E, Schneider B, Buckler ES, Boland W, Gershenzon J, Jander G, Erb M, Kollner TG (2016) Biosynthesis of 8-O-Methylated Benzoxazinoid Defense Compounds in Maize. *Plant Cell* 28: 1682-1700

Pubmed: [Author and Title](#)

CrossRef: [Author and Title](#)

Google Scholar: [Author Only](#) [Title Only](#) [Author and Title](#)

Harborne JB (1999) The comparative biochemistry of phytoalexin induction in plants. *Biochem Syst and Ecol* 27: 335-367

Pubmed: [Author and Title](#)

CrossRef: [Author and Title](#)

Google Scholar: [Author Only](#) [Title Only](#) [Author and Title](#)

Hirsch CN, Foerster JM, Johnson JM, Sekhon RS, Muttoni G, Vaillancourt B, Penagaricano F, Lindquist E, Pedraza MA, Barry K, de Leon N, Kaeppler SM, Buell CR (2014) Insights into the Maize Pan-Genome and Pan-Transcriptome. *Plant Cell* 26: 121-135

Pubmed: [Author and Title](#)

CrossRef: [Author and Title](#)

Google Scholar: [Author Only Title Only Author and Title](#)

Horevaj P, Milus EA, Bluhm BH (2011) A real-time qPCR assay to quantify *Fusarium graminearum* biomass in wheat kernels. J Appl Microbiol 111: 396-406

Pubmed: [Author and Title](#)

CrossRef: [Author and Title](#)

Google Scholar: [Author Only Title Only Author and Title](#)

Huffaker A, Kaplan F, Vaughan MM, Dafoe NJ, Ni X, Rocca JR, Alborn HT, Teal PEA, Schmelz EA (2011) Novel Acidic Sesquiterpenoids Constitute a Dominant Class of Pathogen-Induced Phytoalexins in Maize. Plant Physiol 156: 2082-2097

Pubmed: [Author and Title](#)

CrossRef: [Author and Title](#)

Google Scholar: [Author Only Title Only Author and Title](#)

Huffaker A, Pearce G, Veyrat N, Erb M, Turlings TCJ, Sartor R, Shen Z, Briggs SP, Vaughan MM, Alborn HT, Teal PEA, Schmelz EA (2013) Plant elicitor peptides are conserved signals regulating direct and indirect antiherbivore defense. Proc Natl Acad Sci USA 110: 5707-5712

Pubmed: [Author and Title](#)

CrossRef: [Author and Title](#)

Google Scholar: [Author Only Title Only Author and Title](#)

Iijima Y, Davidovich-Rikanati R, Fridman E, Gang DR, Bar E, Lewinsohn E, Pichersky E (2004) The biochemical and molecular basis for the divergent patterns in the biosynthesis of terpenes and phenylpropenes in the peltate glands of three cultivars of basil. Plant Physiol 136: 3724-3736

Pubmed: [Author and Title](#)

CrossRef: [Author and Title](#)

Google Scholar: [Author Only Title Only Author and Title](#)

Katerinopoulos EH, Isaakidis D, Sofou K, Spyros A (2011) Use of costic acid or extracts of *Dittrichia viscosa* against *Varroa destructor*. In. Google Patents

Pubmed: [Author and Title](#)

CrossRef: [Author and Title](#)

Google Scholar: [Author Only Title Only Author and Title](#)

Kollner TG, Held M, Lenk C, Hiltbold I, Turlings TCJ, Gershenzon J, Degenhardt J (2008) A maize (E)-beta-caryophyllene synthase implicated in indirect defense responses against herbivores is not expressed in most American maize varieties. Plant Cell 20: 482-494

Pubmed: [Author and Title](#)

CrossRef: [Author and Title](#)

Google Scholar: [Author Only Title Only Author and Title](#)

Kollner TG, Lenk C, Schnee C, Kopke S, Lindemann P, Gershenzon J, Degenhardt J (2013) Localization of sesquiterpene formation and emission in maize leaves after herbivore damage. BMC Plant Biol 13:15

Pubmed: [Author and Title](#)

CrossRef: [Author and Title](#)

Google Scholar: [Author Only Title Only Author and Title](#)

Kollner TG, Schnee C, Gershenzon J, Degenhardt J (2004) The sesquiterpene hydrocarbons of maize (*Zea mays*) form five groups with distinct developmental and organ-specific distribution. Phytochem 65: 1895-1902

Pubmed: [Author and Title](#)

CrossRef: [Author and Title](#)

Google Scholar: [Author Only Title Only Author and Title](#)

Kollner TG, Schnee C, Gershenzon J, Degenhardt J (2004) The variability of sesquiterpenes cultivars is controlled by allelic emitted from two *Zea mays* variation of two terpene synthase genes encoding stereoselective multiple product enzymes. Plant Cell 16: 1115-1131

Pubmed: [Author and Title](#)

CrossRef: [Author and Title](#)

Google Scholar: [Author Only Title Only Author and Title](#)

Kollner TG, Schnee C, Li S, Svatos A, Schneider B, Gershenzon J, Degenhardt J (2008) Protonation of a neutral (S)-beta-bisabolene intermediate is involved in (S)-beta-macrocarpene formation by the maize sesquiterpene synthases TPS6 and TPS11. J Biol Chem 283: 20779-20788

Pubmed: [Author and Title](#)

CrossRef: [Author and Title](#)

Google Scholar: [Author Only Title Only Author and Title](#)

Lanubile A, Ferrarini A, Maschietto V, Delledonne M, Marocco A, Bellin D (2014) Functional genomic analysis of constitutive and inducible defense responses to *Fusarium verticillioides* infection in maize genotypes with contrasting ear rot resistance. BMC Genomics 15:710

Pubmed: [Author and Title](#)

CrossRef: [Author and Title](#)

Google Scholar: [Author Only Title Only Author and Title](#)

Lee M, Sharopova N, Beavis WD, Grant D, Katt M, Blair D, Hallauer A (2002) Expanding the genetic map of maize with the intermated B73 x Mo17 (IBM) population. Plant Mol Biol 48: 453-461

Pubmed: [Author and Title](#)
CrossRef: [Author and Title](#)
Google Scholar: [Author Only Title Only Author and Title](#)

Lipka AE, Tian F, Wang QS, Peiffer J, Li M, Bradbury PJ, Gore MA, Buckler ES, Zhang ZW (2012) GAPIT: genome association and prediction integrated tool. *Bioinformatics* 28: 2397-2399

Pubmed: [Author and Title](#)
CrossRef: [Author and Title](#)
Google Scholar: [Author Only Title Only Author and Title](#)

Livak KJ, Schmittgen TD (2001) Analysis of relative gene expression data using real-time quantitative PCR and the 2(T)(-Delta Delta C) method. *Methods* 25: 402-408

Pubmed: [Author and Title](#)
CrossRef: [Author and Title](#)
Google Scholar: [Author Only Title Only Author and Title](#)

McMullen MD, Frey M, Degenhardt J (2009) Genetics and Biochemistry of Insect Resistance in Maize. In JL Bennetzen, SC Hake, eds, *Handbook of Maize: Its Biology*. Springer New York, New York, NY, pp 271-289

Pubmed: [Author and Title](#)
CrossRef: [Author and Title](#)
Google Scholar: [Author Only Title Only Author and Title](#)

McMullen MD, Kresovich S, Villeda HS, Bradbury P, Li H, Sun Q, Flint-Garcia S, Thornsberry J, Acharya C, Bottoms C, Brown P, Browne C, Eller M, Guill K, Harjes C, Kroon D, Lepak N, Mitchell SE, Peterson B, Pressoir G, Romero S, Rosas MO, Salvo S, Yates H, Hanson M, Jones E, Smith S, Glaubitz JC, Goodman M, Ware D, Holland JB, Buckler ES (2009) Genetic Properties of the Maize Nested Association Mapping Population. *Science* 325: 737-740

Pubmed: [Author and Title](#)
CrossRef: [Author and Title](#)
Google Scholar: [Author Only Title Only Author and Title](#)

Meihs LN, Handrick V, Glauser G, Barbier H, Kaur H, Haribal MM, Lipka AE, Gershenzon J, Buckler ES, Erb M, Kollner TG, Jander G (2013) Natural Variation in Maize Aphid Resistance Is Associated with 2,4-Dihydroxy-7-Methoxy-1,4-Benzoxazin-3-One Glucoside Methyltransferase Activity. *Plant Cell* 25: 2341-2355

Pubmed: [Author and Title](#)
CrossRef: [Author and Title](#)
Google Scholar: [Author Only Title Only Author and Title](#)

Meinke LJ, Sappington TW, Onstad DW, Guillemaud T, Miller NJ, Judith K, Nora L, Furlan L, Jozsef K, Ferenc T (2009) Western corn rootworm (*Diabrotica virgifera virgifera* LeConte) population dynamics. *Agric For Entomol* 11: 29-46

Pubmed: [Author and Title](#)
CrossRef: [Author and Title](#)
Google Scholar: [Author Only Title Only Author and Title](#)

Meyer JDF, Snook ME, Houchins KE, Rector BG, Widstrom NW, McMullen MD (2007) Quantitative trait loci for maysin synthesis in maize (*Zea mays* L.) lines selected for high silk maysin content. *Theor Appl Genet* 115: 119-128

Pubmed: [Author and Title](#)
CrossRef: [Author and Title](#)
Google Scholar: [Author Only Title Only Author and Title](#)

Miller NJ, Guillemaud T, Giordano R, Siegfried BD, Gray ME, Meinke LJ, Sappington TW (2009) Genes, gene flow and adaptation of *Diabrotica virgifera virgifera*. *Agric For Entomol* 11: 47-60

Pubmed: [Author and Title](#)
CrossRef: [Author and Title](#)
Google Scholar: [Author Only Title Only Author and Title](#)

Mule G, Susca A, Stea G, Moretti A (2004) A species-specific PCR assay based on the calmodulin partial gene for identification of *Fusarium verticillioides*, *F. proliferatum* and *F. subglutinans*. *Eur J Plant Path* 110: 495-502

Pubmed: [Author and Title](#)
CrossRef: [Author and Title](#)
Google Scholar: [Author Only Title Only Author and Title](#)

Nguyen DT, Gopfert JC, Ikezawa N, MacNevin G, Kathiresan M, Conrad J, Spring O, Ro DK (2010) Biochemical Conservation and Evolution of Germacrene A Oxidase in Asteraceae. *J Bio Chem* 285: 16588-16598

Pubmed: [Author and Title](#)
CrossRef: [Author and Title](#)
Google Scholar: [Author Only Title Only Author and Title](#)

Olukolu BA, Tracy WF, Wissler R, De Vries B, Balint-Kurti PJ (2016) A Genome-Wide Association Study for Partial Resistance to Maize Common Rust. *Phytopathology* 106: 745-751

Pubmed: [Author and Title](#)
CrossRef: [Author and Title](#)
Google Scholar: [Author Only Title Only Author and Title](#)

Rao KV, Alvarez FM (1981) Antibiotic principle of *Eupatorium capillifolium*. *J Nat Prod* 44: 252-256

Pubmed: [Author and Title](#)

CrossRef: [Author and Title](#)

Google Scholar: [Author Only Title Only Author and Title](#)

Rasmann S, Kollner TG, Degenhardt J, Hiltbold I, Toepfer S, Kuhlmann U, Gershenzon J, Turlings TCJ (2005) Recruitment of entomopathogenic nematodes by insect-damaged maize roots. Nature 434: 732-737

Pubmed: [Author and Title](#)

CrossRef: [Author and Title](#)

Google Scholar: [Author Only Title Only Author and Title](#)

Richter A, Schaff C, Zhang Z, Lipka AE, Tian F, Köllner TG, Schnee C, Preiß S, Irmisch S, Jander G, Boland W, Gershenzon J, Buckler ES, Degenhardt J (2016) Characterization of Biosynthetic Pathways for the Production of the Volatile Homoterpenes DMNT and TMTT in Zea mays. Plant Cell 28: 2651-2665

Pubmed: [Author and Title](#)

CrossRef: [Author and Title](#)

Google Scholar: [Author Only Title Only Author and Title](#)

Saba F (1970) Host plant spectrum and temperature limitations of Diabrotica balteata. Canad Entomol 102: 684-8

Pubmed: [Author and Title](#)

CrossRef: [Author and Title](#)

Google Scholar: [Author Only Title Only Author and Title](#)

Samayoa LF, Malvar RA, Olukolu BA, Holland JB, Butron A (2015) Genome-wide association study reveals a set of genes associated with resistance to the Mediterranean corn borer (Sesamia nonagrioides L.) in a maize diversity panel. BMC Plant Biol 15:35

Pubmed: [Author and Title](#)

CrossRef: [Author and Title](#)

Google Scholar: [Author Only Title Only Author and Title](#)

Schmelz EA, Alborn HT, Tumlinson JH (2001) The influence of intact-plant and excised-leaf bioassay designs on volicitin- and jasmonic acid-induced sesquiterpene volatile release in Zea mays. Planta 214: 171-179

Pubmed: [Author and Title](#)

CrossRef: [Author and Title](#)

Google Scholar: [Author Only Title Only Author and Title](#)

Schmelz EA, Engelberth J, Alborn HT, Tumlinson JH, Teal PEA (2009) Phytohormone-based activity mapping of insect herbivore-produced elicitors. Proc Natl Acad Sci USA 106: 653-657

Pubmed: [Author and Title](#)

CrossRef: [Author and Title](#)

Google Scholar: [Author Only Title Only Author and Title](#)

Schmelz EA, Engelberth J, Tumlinson JH, Block A, Alborn HT (2004) The use of vapor phase extraction in metabolic profiling of phytohormones and other metabolites. Plant J 39: 790-808

Pubmed: [Author and Title](#)

CrossRef: [Author and Title](#)

Google Scholar: [Author Only Title Only Author and Title](#)

Schmelz EA, Huffaker A, Sims JW, Christensen SA, Lu X, Okada K, Peters RJ (2014) Biosynthesis, elicitation and roles of monocot terpenoid phytoalexins. Plant J 79: 659-678

Pubmed: [Author and Title](#)

CrossRef: [Author and Title](#)

Google Scholar: [Author Only Title Only Author and Title](#)

Schmelz EA, Kaplan F, Huffaker A, Dafoe NJ, Vaughan MM, Ni X, Rocca JR, Alborn HT, Teal PE (2011) Identity, regulation, and activity of inducible diterpenoid phytoalexins in maize. Proc Natl Acad Sci USA 108: 5455-5460

Pubmed: [Author and Title](#)

CrossRef: [Author and Title](#)

Google Scholar: [Author Only Title Only Author and Title](#)

Schnee C, Kollner TG, Gershenzon J, Degenhardt J (2002) The maize gene terpene synthase 1 encodes a sesquiterpene synthase catalyzing the formation of (E)-beta-farnesene, (E)-nerolidol, and (E,E)-farnesol after herbivore damage. Plant Physiol 130: 2049-2060

Pubmed: [Author and Title](#)

CrossRef: [Author and Title](#)

Google Scholar: [Author Only Title Only Author and Title](#)

Schnee C, Kollner TG, Held M, Turlings TCJ, Gershenzon J, Degenhardt J (2006) The products of a single maize sesquiterpene synthase form a volatile defense signal that attracts natural enemies of maize herbivores. Proc Natl Acad Sci USA 103: 1129-1134

Pubmed: [Author and Title](#)

CrossRef: [Author and Title](#)

Google Scholar: [Author Only Title Only Author and Title](#)

Sowbhagya HB (2014) Chemistry, technology, and nutraceutical functions of celery (Apium graveolens L.): an overview. Crit Rev Food Sci Nutr 54: 389-398

Pubmed: [Author and Title](#)

CrossRef: [Author and Title](#)

Google Scholar: [Author Only Title Only Author and Title](#)

Spencer JL, Hibbard BE, Moeser J, Onstad DW (2009) Behavior and ecology of the western corn rootworm (Diabrotica virgifera

virgifera LeConte). *Agricul For Entomol* 11: 9-27

Pubmed: [Author and Title](#)

CrossRef: [Author and Title](#)

Google Scholar: [Author Only](#) [Title Only](#) [Author and Title](#)

Starks CM, Back KW, Chappell J, Noel JP (1997) Structural basis for cyclic terpene biosynthesis by tobacco 5-epi-aristolochene synthase. *Science* 277: 1815-1820

Pubmed: [Author and Title](#)

CrossRef: [Author and Title](#)

Google Scholar: [Author Only](#) [Title Only](#) [Author and Title](#)

Tinsley NA, Estes RE, Gray ME (2013) Validation of a nested error component model to estimate damage caused by corn rootworm larvae. *J Appl Entomol* 137: 161-169

Pubmed: [Author and Title](#)

CrossRef: [Author and Title](#)

Google Scholar: [Author Only](#) [Title Only](#) [Author and Title](#)

Turlings TCJ, Tumlinson JH, Lewis WJ (1990) Exploitation of herbivore-induced plant odors by host-seeking parasitic wasps. *Science* 250: 1251-1253

Pubmed: [Author and Title](#)

CrossRef: [Author and Title](#)

Google Scholar: [Author Only](#) [Title Only](#) [Author and Title](#)

Turner SD (2014) qqman: an R package for visualizing GWAS results using QQ and Manhattan plots. Preprint at bioRxiv <http://dx.doi.org/10.1101/005165>

Pubmed: [Author and Title](#)

CrossRef: [Author and Title](#)

Google Scholar: [Author Only](#) [Title Only](#) [Author and Title](#)

Vanetten HD, Mansfield JW, Bailey JA, Farmer EE (1994) 2 Classes of plant antibiotics - phytoalexins versus phytoanticipins. *Plant Cell* 6: 1191-1192

Pubmed: [Author and Title](#)

CrossRef: [Author and Title](#)

Google Scholar: [Author Only](#) [Title Only](#) [Author and Title](#)

VanRaden PM (2008) Efficient Methods to Compute Genomic Predictions. *J Dairy Sci* 91: 4414-4423

Pubmed: [Author and Title](#)

CrossRef: [Author and Title](#)

Google Scholar: [Author Only](#) [Title Only](#) [Author and Title](#)

Vaughan MM, Christensen S, Schmelz EA, Huffaker A, McAuslane HJ, Alborn HT, Romero M, Allen LH, Teal PEA (2015) Accumulation of terpenoid phytoalexins in maize roots is associated with drought tolerance. *Plant Cell Environ* 38: 2195-2207

Pubmed: [Author and Title](#)

CrossRef: [Author and Title](#)

Google Scholar: [Author Only](#) [Title Only](#) [Author and Title](#)

Wu QX, Shi YP, Jia ZJ (2006) Eudesmane sesquiterpenoids from the Asteraceae family. *Nat Prod Rep* 23: 699-734

Pubmed: [Author and Title](#)

CrossRef: [Author and Title](#)

Google Scholar: [Author Only](#) [Title Only](#) [Author and Title](#)

Yan J, Lipka AE, Schmelz EA, Buckler ES, Jander G (2015) Accumulation of 5-hydroxynorvaline in maize (*Zea mays*) leaves is induced by insect feeding and abiotic stress. *J Exp Bot* 66: 593-602

Pubmed: [Author and Title](#)

CrossRef: [Author and Title](#)

Google Scholar: [Author Only](#) [Title Only](#) [Author and Title](#)

Yu JM, Pressoir G, Briggs WH, Bi IV, Yamasaki M, Doebley JF, McMullen MD, Gaut BS, Nielsen DM, Holland JB, Kresovich S, Buckler ES (2006) A unified mixed-model method for association mapping that accounts for multiple levels of relatedness. *Nat Genet* 38: 203-208

Pubmed: [Author and Title](#)

CrossRef: [Author and Title](#)

Google Scholar: [Author Only](#) [Title Only](#) [Author and Title](#)

Zhang ZW, Ersoz E, Lai CQ, Todhunter RJ, Tiwari HK, Gore MA, Bradbury PJ, Yu JM, Arnett DK, Ordovas JM, Buckler ES (2010) Mixed linear model approach adapted for genome-wide association studies. *Nat Genet* 42: 355-U118

Pubmed: [Author and Title](#)

CrossRef: [Author and Title](#)

Google Scholar: [Author Only](#) [Title Only](#) [Author and Title](#)